science.sciencemag.org/content/366/6462/246/suppl/DC1

Supplementary Materials for

Shisa7 is a $GABA_A$ receptor auxiliary subunit controlling benzodiazepine actions

Wenyan Han, Jun Li*, Kenneth A. Pelkey*, Saurabh Pandey, Xiumin Chen, Ya-Xian Wang, Kunwei Wu, Lihao Ge, Tianming Li, David Castellano, Chengyu Liu, Ling-Gang Wu, Ronald S. Petralia, Joseph W. Lynch, Chris J. McBain, Wei Lu†

*These authors contributed equally to this work.
†Corresponding author. Email: luw4@mail.nih.gov

Published 11 October 2019, *Science* **366**, 246 (2019)

DOI: 10.1126/science.aax5719

This PDF file includes:

Other Supplementary Material for this manuscript includes the following:
(available at science.sciencemag.org/content/366/6462/246/suppl/DC1)

Supplementary Discussion

We found that among the three Shisa subfamily proteins (i.e. Shisa6,7,9), the distinct localization of Shisa7 at GABAergic synapses requires a unique GRID domain in the Shisa7 N-terminus that mediates its interaction with $GABA_A$Rs. Thus, although all three Shisas contain the AMPAR binding motif in their C-termini and can interact with AMPAR subunits in heterologous cells when they were co-transfected (*26*), Shisa7 with the GRID motif is located at GABAergic synapses and associates with $GABA_A$Rs. Furthermore, STED super-resolution microscopy and a cell adhesion assay supported a direct interaction between Shisa7 and $GABA_A$Rs. Our data are consistent with a recent proteomic study showing that Shisa7 is in complex with native $GABA_A$Rs in the brain (*14*). A recent study showed that after prolonged viral overexpression in hippocampal neurons (over one week), tagged Shisa7 co-localized with Homer1, and that Shisa7 in the brain interacted with AMPARs (*27*). However, our work demonstrates that Shisa7 does not co-localize with GluA1, Homer1, PSD-95 or vGluT1. In addition, native Shisa7 in neurons largely co-localizes with gephyrin and $GABA_A$Rs, and interacts with $GABA_A$Rs, but not AMPARs. Currently, the reason for the discrepancies is unclear. Notably, in the previous study (*27*), the authors reported in the Author Reponses that prolonged overexpression of Shisa7 (over one week) resulted in a loss of spines and thus excluded a meaningful analysis of Shisa7-PSD-95 co-localization (*27*). The reason for the loss of spines after prolonged overexpression of Shisa7 as reported before (*27*) remains unknown. In our study, subcellular localizations of tagged Shisa7 in WT and KO neurons were performed under the expression condition of less than 24 hrs.

Our finding that Shisa7 interacts with α1, α2 or γ2, but not β2 or β3, indicates subunit specificity and a possible variable stoichiometry of the Shisa7-$GABA_A$R complex. Intriguingly, although β3 on its own does not interact with Shisa7, it appears to be involved in the regulation of trafficking and DZ sensitivity of $GABA_A$Rs by Shisa7. It is worth noting that while the classic BDZ binding site of the $GABA_A$R is located at the α and γ subunit interface (*1, 9*), a secondary BDZ modulating site involving the β subunit has been proposed (*28-30*). An important role of the β3 subunit in mediating the BDZ hypnotic effect in mice has also been reported (*31*). Thus, the role of the β3 subunit in Shisa7 regulation of $GABA_A$Rs warrants future investigation that will provide structural insights into Shisa7 modulation of $GABA_A$Rs. One notable observation is that Shisa7 increased the DZ-induced potentiation of $\alpha1\beta3\gamma2$, but not $\alpha1\beta2\gamma2$, in HEK cells. Although $\alpha1\beta2\gamma2$ is considered to be the most abundant $GABA_A$Rs in the brain (*2*), association of endogenous β3 with α1 can be readily detected (*15*), and thus it is possible that $\alpha1\beta3\gamma2$ could be involved in DZ actions observed in the current study. Future experiments to further characterize the potential role of $\alpha1\beta3$-containing receptors *in vivo* will be critical. It is worth noting that although our electrophysiological experiments were performed in hippocampal CA1 neurons, the regulation of the DZ effects on mouse behavior by Shisa7 may not be necessarily mediated by this brain region (*10*). Thus, future work toward a more complete understanding of Shisa7 in different types of neurons will be important. It is also worth mentioning that our Shisa7 WT and KO mice are mixed C57BL/6J/N, and thus it cannot be formally excluded that some differences of behavioral observations might be due to the differential expression of the $GABA_A$R α2 subunit from different mouse strains (*32*). In addition, in some of the behavioral experiments, we used a clinical grade of DZ containing ethanol. Correspondingly, the vehicle as the control also included ethanol. Furthermore, DZ dissolved in vehicle without ethanol produced similar effects on LORR as the clinical grade DZ.

Previous studies have demonstrated the differential roles of $GABA_A$R subtypes in mediating anxiolytic-like and sedative effects of BDZs *in vivo* (*21-23*). Indeed, α1-containing receptors have been implicated in sedative effects of BDZs (*21, 22*), and α2-containg receptors are critical for

BDZ anxiolysis (*23*). However, the exact roles of α1- and α2- containing receptors in mediating hypnotic action of BDZs remain unclear. In α1 global KO mice, the duration of LORR induced by diazepam was paradoxically increased, likely due to compensatory adaptations of other $GABA_AR$ subunits (*33*), but LORR induced by flurazepam was reduced (*34*). It has been shown that both β2- and β3- containing receptors are critical for the hypnotic effect of the general anesthetic etomidate (*34, 35*). Since $\alpha1\beta2\gamma2$ and $\alpha2\beta3\gamma2$ are the abundant $GABA_AR$ species in the brain, it is plausible that both α1- and α2- containing receptors may contribute to BDZ hypnosis.

Currently the mechanisms underlying the regulation of trafficking and DZ sensitivity of $GABA_ARs$ by Shisa7 are unclear. The fact that both total expression and surface expression levels as well as synaptic abundance of several $GABA_AR$ subunits are reduced in Shisa7 KO hippocampi indicates that Shisa7 may regulate stability, trafficking and/or synaptic targeting of $GABA_ARs$. In addition, the Shisa7 regulation of $GABA_ARs$ is reminiscent of AMPA receptor (AMPAR) auxiliary subunits that affect almost every aspect of AMPAR trafficking and function (*36-39*). Discovery and investigation of AMPAR auxiliary subunits have revolutionized our understanding of AMPAR function and changed the way we think about ionotropic glutamate receptors (*36-39*). Thus, future work toward a more complete understanding of Shisa7 in control of $GABA_AR$ trafficking and function will be invaluable to our understanding of $GABA_AR$ biology, physiology and pathology.

Materials and Methods

Animals

All animal handling was performed in accordance with animal protocols approved by the Institutional Animal Care and Use Committee (IACUC) at NIH/NINDS and NIH/NICHD. Adult C57BL/6J mice (6-8 weeks old) were purchased from the Jackson Laboratory, and were housed and bred in a conventional vivarium with *ad libitum* access to food and water under a 12-hr circadian cycle. The day of vaginal plug detection was designated as embryonic day 0.5 (E0.5) and the day of birth as postnatal day 0 (P0). Timed-pregnant mice at E14.5-15.5 were used for *in utero* electroporation (IUE). Timed-pregnant C57BL/6J mice at E17.5-18.5 were used for cultures of primary hippocampal neurons. Mice of either sex were used and were randomly assigned for all experiments unless otherwise specified.

Generation of *Shisa7*$^{-/-}$ mice

The Shisa7 germline knockout (KO) mice were generated using CRISPR/Cas9 technology with two single-guide RNAs (sgRNAs) that specifically target to nucleotide sequences of Exon 2 (TGCGGAGGCTAGCAGCGCGA) and Exon 6 (CTGGATGTCTGATGCGGGCG) in Shisa7 genomic DNA on the C57BL/6N background. When co-microinjected, these sgRNAs can delete the entire region between the two cutting sites. These sgRNAs were generated using an *in vitro* transcription service (ThermoFisher), and the donor oligos were purchased from IDT. Cas9 mRNA (100 ng/μl, purchased from TriLink Biotechnologies) and corresponding sgRNAs (20 ng/μl each), were co-microinjected into fertilized eggs collected from C57BL/6N mice (Charles River). The injected zygotes were cultured overnight in M16 medium at 37°C in 5% CO_2. The next morning, embryos that had reached the 2-cell stage of development were implanted into the oviducts of pseudo-pregnant foster mothers (Swiss Webster, Taconic Farm). The mice born to the foster mothers were genotyped using PCR and DNA sequencing and the founder mice with expected Shisa7 deletions were bred to C57BL/6J mice for establishing knockout mouse lines. Genotyping tests of offspring were performed (Exon2-Forward: 5'-ACTTCTGTATCCCCTCCTCCGTC-3'; Exon6-Forward: 5'-TGAGGCGCTTCGCCAGAGTCGCGAG-3'; Exon6-Reverse: 5'-CAGAGCCTTGGTGTGTATGATAAGC-3') by general PCR. The genotypic group *Shisa7*$^{+/+}$, *Shisa7*$^{+/-}$ and *Shisa7*$^{-/-}$ indicated wild-type (WT), heterozygous (Het) and homozygous (Homo) KO for *Shisa7*, respectively. Littermates of WT and KO mice at P15-18 were used for electrophysiology experiments. Adult littermates of WT and KO mice (6-8 weeks old, C57BL/6J/N) were used for behavioral, biochemical and electron microscopic experiments, and only male mice were used in behavioral tests. Timed-pregnant WT and Shisa7 KO mice at E17.5-18.5 were used for hippocampal neuron culture.

Plasmids

Mouse Shisa7 cDNA was purchased from NovoPro (Cat#: 739321-1) and cloned into pCAGGs-IRES-GFP vector and pcDNA3.0 vector, respectively. Shisa6 and Shisa9 cDNAs were gifts from Jakob von Engelhardt's lab and were cloned into pcDNA3.0 vector. N-terminal HA-tag of Shisa6, Shisa7 and Shisa9 were separately cloned into pcDNA3.0. The coding sequence of Shisa7 and Shisa9 N- and C- terminal swap mutants were generated using pcDNA-HA-Shisa7 and pcDNA-HA-shisa9 as templates by overlapping PCR and inserted into pcDNA3.0 vector. The miniprep of Shisa7 CRISPR sgRNAs #1 (ACCAAGACCAGCCCCGCGAG), #2 (GGCTGTTGACGTTGTAGTGC) and #3 (CAAGCACCACGCCGCCACAC) were generated in GenScript, and the sgRNA was inserted into pSpCas9-BB-2A-GFP (PX458) vector at the SacI cutting site. The coding sequence of Shisa7 point mutations for sgRNA$^{\#1}$ resistant plasmid (mutation region: ACCAAGACCAGCCCCGCGAG to ACCAAAACATCCCCAGCGAG) was cloned by overlapping PCR and inserted into pCAGGs-IRES-mCherry vector. N-terminal Flag-tagged Shisa7 was cloned into pcDNA3.0 (pcDNA3-Flag-Shisa7). The coding sequence of Shisa7

$\Delta N_{154/175}$ deletion and ΔC-tail mutants were separately generated by overlapping PCR using pcDNA3-Flag-Shisa7 as a template and inserted into the pcDNA3.0 vector. Untagged human $GABA_AR$ α1 (accession No.: NM_000806.5), α2 (accession No.: NM_000807.3) and γ2L (accession No.: NM_198903.2) in pcDNA3.1 Zeo+, and pAAV-Syn-Flag-Shisa7 was generated using backbone pAAV-Syn-GFP (Addgene: 58867) by GenScript (GenScript, Piscataway, NJ). Gephyrin plasmid was purchased from Addgene (Cat#: 68815). Mouse Tmem132b and Neuroligin2 were cloned into pCAGGs-IRES-GFP vector, and mouse Lhfpl4(GARLH4), Prrt2, Kctd12 and Shisa9 were cloned into pCAGGs-IRES-GFP vector by GenScript. Human $GABA_AR$ β2 and β3 in pcDNA3.1 Zeo were gifts from Joseph Lynch's lab at University of Queensland, Australia. $GABA_AR$ α3 was a gift from Derek Bowie's lab at McGill University. pCAGGs-HA-Neuroligin2-IRES-mCherry plasmid was a gift from Roger Nicoll's lab at UCSF. All constructs were verified by DNA sequencing.

Antibodies

Anti-Shisa7 polyclonal antibody was raised in rabbit against sequence GTLARRPPFQRQGT (position 519–532 in mouse Shisa7) (GenScript; Piscataway, NJ). The antibody was affinity-purified against the antigenic peptide, suspended at 0.5 mg/mL in PBS containing 0.02% NaN3, and stored at -20°C. Anti-Shisa7 monoclonal antibody was produced in mice against sequence TTPPPLAGGAGGAGGAGGGPGPGQAGWLEGG (position 141-171 in mouse Shisa7, Mab7C10), suspended at 0.9 mg/mL in PBS containing 0.02% NaN3, and stored at -20°C (GenScript; Piscataway, NJ). Immunoblot or immunocytochemistry were performed to validate the custom Shisa7 rabbit and mouse antibodies using WT and Shisa7 KO mice. For validation of Shisa7 sgRNAs and the sgRNA resistant plasmid, anti-Flag (1:500, MilliporeSigma, F1804, mouse) and anti-Tubulin (1:5000, MilliporeSigma, T8203, mouse) were used. Antibodies used for co-IP of $GABA_ARs$ in hippocampal lysates were: anti-Shisa7 (GenScript, Rabbit, polyclonal), anti-GluA1 (MilliporeSigma, AB1504, Rabbit), anti-α1 (MilliporeSigma, 06-868, rabbit) and anti-α2 (Guinea pig) antibodies. Immunoblot: anti-Shisa7 (1:500, GenScript, Rabbit, polyclonal), anti-α1: (1:1000, NeuroMab, N95/35, mouse), anti-α2 (1:1000, NeuroMab, N399-19, mouse), anti-GluA1(1:1000, MilliporeSigma, MAB2263, mouse) and anti-γ2 (1:500, MilliporeSigma, MABN263, mouse). Antibodies used for co-IP in HEK-293T (HEK) cells were: anti-Flag (Sigma-Aldrich, F7425, rabbit), anti-α1 (1:1000, Synaptic systems, 224203, rabbit), anti-α2 (1:1000, NeuroMab, N399-19, mouse), anti-β2 (1:1000; SigmaMillipore, AB5561), anti-β3 (1:500; SigmaMillipore, SAB2100880, rabbit) and γ2 (1:1000, Synaptic systems, 224003, rabbit). Antibodies used for immunoblotting in hippocampal lysates were: anti-Shisa7 (1:500, GenScript, Rabbit), anti-α1: (1:1000, NeuroMab, N95/35, mouse), anti-α2 (1:1000, NeuroMab, N399-19, mouse), anti-α3 (1:1000, Synaptic systems, 224303, rabbit), anti-β2 (1:1000; SigmaMillipore, AB5561), anti-β3 (1:500; SigmaMillipore, SAB2100880, rabbit), anti-γ2 (1:1000, Synaptic systems, 224003, rabbit), gephyrin: 1:1000, Synaptic systems, 147111, anti-vGAT (1:1000, Synaptic systems, 131002, rabbit), anti-PSD-95 (1:1000, NeuroMab, K28/43, mouse) and anti-vGluT1 (1:1000, Synaptic system, 135302, rabbit), anti-GluA1(1:1000, MilliporeSigma, MAB2263, mouse), anti-GluN1(1:1000, MilliporeSigma, 05-432, mouse). Antibodies used for immunocytochemistry in cultured neurons were: anti-HA (1:1000, Santa Cruz, sc-805, rabbit) or anti-HA: (1:1000, Santa Cruz, sc-7392, mouse), anti-Flag (1:1000, MilliporeSigma, F2555, rabbit), anti-MAP2 (1:1000, Aves Labs, MAP, chicken), anti-gephyrin (1:1000, Synaptic systems, 147021, mouse), anti-vGAT (1:1000, Synaptic systems, 131002, rabbit), anti-PSD-95 (1:1000, NeuroMab, K28/43, mouse), anti-vGluT1 (1:1000, Synaptic system, 135302, rabbit) and anti-Homer1 (1:1000, synaptic systems, 160004, guinea pig), anti-Flag (1:500, MilliporeSigma, F1804, mouse), anti-GluA1 (1:1000, MAB2263, rabbit), anti-Shisa7 (1:500, Mab7C10,mouse), anti-α2: (1:1000; Synaptic system, 224104, guinea pig), anti-α1: (1:1000, Synaptic system, 224205, guinea pig), anti-γ2 (surface: 1:1000, Synaptic systems, 224003). Antibodies used for immunocytochemistry in HEK

cells were: anti- β2 or β3 (surface: 1:1000, SigmaMillipore, MAB341, mouse; total: β2: 1:1000; SigmaMillipore, AB5561, rabbit; β3: 1:500; SigmaMillipore, SAB2100880, rabbit), anti-α2 (surface: 1:1000; Synaptic system, 224103, rabbit) antibodies; total: anti-α2: (1:1000; Synaptic system, 224104, guinea pig) and anti-Flag (1:1000, Sigma, F1804, mouse). Antibodies used for surface and total labeling of $GABA_A$Rs in neurons were: anti-α1 (surface: 1:1000, Synaptic systems, 224203, rabbit; total: 1:1000, Synaptic system, 224205, guinea pig), anti-α2 (surface: 1:1000, Synaptic systems, 224103, rabbit; total: 1:1000, Synaptic system, 224104, guinea pig), anti-γ2 (surface: 1:1000, Synaptic systems, 224003, rabbit; total: 1:1000, Synaptic system, 224004, guinea pig) and anti-GFP (Roche, 11814460001, mouse).

***In situ* hybridization (ISH)**

Cultured hippocampal neurons expressing Shisa7 sgRNA$^{\#1}$ or sgRNA$^{\#2}$ electroporated at E14.5 were fixed in fixation buffer (4% PFA in 1x PBS) at room temperature (RT) for 15 min at DIV16. Coverslips were then washed three times with 1x PBS and sequentially incubated in 50, 70, and 100% ethanol for 5 min for dehydration. The coverslips were then submerged in 70 and 50% ethanol for 2 min for rehydration followed by incubation in 1x PBS for 10 min. The coverslips were then treated with hydrogen peroxide and protease III (1:15 diluted in 1x PBS) (RNAscope, 2000258) for 10 min followed by washing twice in 1x PBS. The coverslips were quickly transferred to the barriered SuperFrost Plus slide (Fisher Scientific, #12-550-15). All of the above steps were performed at RT.

For Shisa7 WT and KO mouse brain ISH, 6-8 weeks old Shisa7 WT and KO littermates were perfused with pre-warmed 4% PFA in 0.1 M phosphate buffer (PB) (~28°C). After post-fixation for 2 hrs at 4°C and washings, the brain was immersed in 30% sucrose in 0.1 M PB for > 24 hrs until the tissue sunk to the bottom of the container at 4°C. The dehydrated brain was placed in a container filled with OCT embedding media and stored at -80°C. The embedded brain was equilibrated at -20°C for 30 min in a cryostat before sectioning. Sagittal slices were sectioned at 14 µm and mounted on SuperFrost® Plus slide. After air drying for 20 min at -20°C, the slide was then washed with 1x PBS to remove OCT and then 2-4 drops of hydrogen peroxide were added for 10 min at RT. The washed slide was then transferred and submerged into the boiled target retrieval solution (RNAscope, 322000) for 5 min. The hot slide was then immediately transferred into distilled water and washed twice, then submerged in fresh 100% EtOH by moving the rack up and down 3-5 times. After air drying, the slide was put in a slide rack and added 2-4 drops of RNAscope® Protease Plus. The rack was then incubated at 40°C for 30 min followed by 3x washings of slides with washing buffer (RNAscope, 320091).

For running the detection protocol, the following steps were done using the RNAscope ® 2.5 HD Detection Kit (Red) User Manual Part 2 (Document No. 322360-USM). Briefly, 4 drops (~50-80 µl) of Shisa7 probe (RNAscope, 483301) solution were added to submerge the coverslip, and then the slide was incubated in a humidity control tray at 40°C for 2 h followed by washing twice in 1x washing buffer for 2 min at RT. The slide was then sequentially incubated with detection reagents AMP1-6 and Fast RED reagent (A:B, 1:60 ratio, RNAscope, 2000173). After rinsing in 1x washing buffer, the slide was removed from the humidity control tray and dried in a dry oven at 60°C for 20 min. For cultured hippocampal neurons, the coverslips containing the neurons were mounted with 3 drops of DAPI Fluoromount-G (SouthernBiotech, 0100-20) without air bubbles. For Shisa7 WT or KO mouse sagittal slices, the slide was dipped in fresh xylene solution followed by DAPI Fluoromount-G, then gently covered with a 24 mm x 50 mm coverslip without air bubbles.

Positive punctate mRNA signal in cultured neurons was detected with a confocal microscope (Zeiss, LSM 880) using a 63x oil objective. The staining of ISH was categorized into five grades based on the recommendation from manufacturer (322360-USM) as described before (*40*).

Briefly, staining scores were defined by the following criteria: 0, no staining or less than 1 dot per 10 neurons; 1, 1–3 dots per neuron; 2, 4–10 dots per neuron, very few dot clusters; 3, >10 dots per neuron, less than 10% positive neurons have dot clusters; 4, >10 dots per neuron, more than 10% positive neurons have dot clusters. And the fluorescent intensity of red Shisa7 positive punctate mRNA signal was analyzed in ImageJ (v 1.51s).

Primary Hippocampal Neuron culture

Primary cultures of hippocampal neurons were prepared as described previously (*41*). Briefly, timed-pregnant mice at E17.5-18.5 were anesthetized on ice and decapitated. The fetal hippocampi were quickly dissected out in ice-cold Hank's balanced salt solution, triturated with a sterile tweezer, and digested with papain (Worthington, LK003176) solution at 37°C for 30 min. After centrifugation for 5 min at 800 r.p.m. at RT, the pellet was resuspended in DNase I-containing Hank's solution, and then was mechanically dissociated into single cells by gentle pipetting up and down. Cells were then transferred into Hank's solution mixed with trypsin inhibitor (10 mg/ml, Sigma, T9253) and BSA (10 mg/ml, Sigma, A9647), and centrifuged at 800 r.p.m. for 10 min. The pellet was resuspended in neurobasal plating media containing 2% fetal bovine serum (FBS) (Gibco, 10437-028), 2% B27 supplements and L-glutamine (2 mM). Neurons were plated at a density of ~8 x 10^4 cells/well on poly-D-lysine (Sigma, P6407) -coated 12 mm glass coverslips residing in 24-well plates for *in situ* hybridization and immunocytochemistry. Culture media were changed by half volume with neurobasal maintenance media containing 2% B27 (GIBCO, 17504-044) supplements and L-glutamine (2 mM) once a week.

***In Utero* electroporation**

A timed-pregnant C57/B6 mouse at ~E14.5-15.5 was anesthetized with 2% isoflurane. The abdominal cavity was cut open and embryos in the uterine horns were gently exposed. The lateral ventricle of the embryo was manually injected with ~1.5-2 µl of plasmid DNA (final concentration: 2 µg/µl; the ratio of Shisa7 sgRNA resistant plasmid Shisa7* vs sgRNA$^{\#1}$ = 1:5) mixed with 0.05% fast green (Sigma 68724). The injection glass pipettes were beveled with the BV-10 micropipette Beveller (Sutter Instrument) before injection. After each injection, voltage steps via tweezer-trodes (5 mm round, platinum electrodes and BTX electroporator, BTX, ECM 830) positioned on either side of the head were applied across the uterus to target hippocampal neural progenitors. Voltage was 45 V for 5 pulses at 1 Hz, each pulse lasting 50 ms. The embryos were moistened with warmed sterile saline and gently moved back to the abdominal cavity. Buprenex (0.1 mg/kg) was applied before sewing and two days after surgery. The electroporated embryos were used for either cultured hippocampal neurons at E17.5-18.5 or hippocampal acute slice preparations at indicated postnatal days for electrophysiological assays.

Immunocytochemistry

Immunocytochemistry in HEK cells. The HEK cell line was purchased from Life Technologies. HEK cells were grown and maintained in DMEM (GIBCO, 10569-010) supplemented with 10% FBS, 1% Pen/Strep and 1% L-glutamine in a humidified atmosphere in a 37°C incubator with 5% CO_2. Transfection was performed in 24-well plates or 6 cm dishes with indicated cDNAs using CalPhos™ Mammalian Transfection Kit (Takara, Cat: 631312) following the manufacturer's instructions. Transfected HEK cells were used for biochemical and immunocytochemistry experiments.

For surface and total $GABA_AR$ β2 or β3 labeling, HEK cells were co-transfected with a ratio of 1:1:3:1 (α:β:γ2L:GFP) using calcium phosphate transfection. 48 hrs after transfection, HEK cells were first live stained with β2 or β3 antibodies in conditioned media in the incubator with 5% CO_2 at 37°C for 30 min. For surface and total $GABA_AR$ α2 labeling, HEK cells were first live stained

with anti- Flag and α2 antibodies in conditioned media at 37°C for 1 hr. Coverslips were then washed 3 times with 1x PBS, and then fixed for 15 min with prewarmed fixation buffer (1% paraformaldehyde and 4% sucrose in 1x PBS, pH 7.4), followed by permeabilization with 0.2% Triton X-100 in PBS for 15 min. The coverslips were then washed and blocked with 5% normal goat serum (in 1x PBS) for 45 min at 37°C, and then incubated with primary α2, β2 or β3 antibodies for total labeling followed by washing 3x 10 min with 1x PBS and Alexa conjugated secondary antibodies (ThermoFisher, 1:1000) for 1 hr at 37°C. After washing, coverslips were mounted with DAPI Fluoromount-G.

For surface Flag-Shisa7 and $GABA_AR$ α2 subunit labeling using Airyscan and STED, HEK cells on the coverslips (#1.5, 25 mm) were co-transfected with a ratio of 1:1:3:1 (α:β:γ2L:Flag-Shisa7) using calcium phosphate transfection. 48-hr after transfection, HEK were first live stained with anti-Flag and anti-α2 antibodies in conditioned media at 37°C for 1 hr. Coverslips were then washed 3 times with 1x PBS, and fixed for 15 min with pre-warmed fixation buffer (1% paraformaldehyde and 4% sucrose in 1x PBS, pH 7.4). After washing, the coverslips were incubated with Alexa conjugated 594 affinipure goat anti-mouse (for sFlag-Shisa7, Jackson ImmunoResearch, 115-585-003) and Atto 647N goat anti-Rabbit (for sα2, Active Motif, #15048) secondary antibodies in 5% normal goat serum (in 1x PBS) for 1 hr at 37°C. After washing, coverslips were mounted with prolong glass antifade mountant with NucBlue stain (Invitrogen, P36981).

Immunocytochemistry in neurons. For co-localization of Shisa family members with synaptic markers, HA-tagged Shisa6, Shisa7, Shisa9 or AAV-syn1-Flag-Shisa7 were transfected into cultured hippocampal neurons at DIV15 using Lipofectamine 3000 (ThermoFisher, L3000015). 24 hrs after transfection, coverslips were fixed in fixation buffer (4% PFA + 4% Sucrose in 1x PBS) for 15 min followed by overnight incubation of HA, MAP2 and gephyrin/vGAT/PSD-95/vGluT1 primary antibodies with 3% NGS and 0.2% Triton X-100 in 1x PBS. For co-localization of Shisa7 with double synaptic markers (Homer1/gephyrin or Homer1/PSD-95), HA-Shisa7 was transfected into cultured hippocampal neurons at DIV15 using Lipofectamine 3000. 24 hrs after transfection, coverslips were fixed for 15 min and followed by washing and overnight incubation of HA, MAP2 and Homer1 together with gephyrin or PSD-95 antibodies with 3% NGS and 0.2% Triton X-100 in 1x PBS at 4°C. After overnight incubation, coverslips were washed 5 min in 1x PBS for three times and then were incubated with secondary antibodies for 1 hr at RT. Coverslips were then washed 5 min in 1x PBS for three times and mounted without bubbles.

For labeling of surface and total endogenous $GABA_AR$ α1, α2 and γ2 subunits in hippocampal neurons, time-pregnant mouse embryos were electroporated with indicated $sgRNA^{\#1}$ or $sgRNA^{\#2}$ into embryonic hippocampal progenitor neurons at E14.5 and cultured at E17.5. Coverslips containing neurons were fixed at DIV16 in fixation buffer for 15 min at RT followed by washing and surface labeling with primary antibodies of α1, α2 or γ2 in 1x PBS with 5% NGS for 5 hrs at RT. After washing, cells on coverslips were incubated with primary antibodies of α1, α2 or γ2 together with MAP2 and GFP in 1x PBS with 3% NGS and 0.2 % Triton X-100 for overnight to label total proteins at 4°C. After overnight incubation, coverslips were washed 5 min in 1x PBS for three times and then were incubated in secondary antibodies for 1 hr at RT followed by 3x 5-min washes and mounting. A similar procedure was performed to label surface and total $GABA_AR$ α1, α2 and γ2 subunits in cultured Shisa7 WT and KO hippocampal neurons at DIV16.

For labeling of surface $GABA_AR$ α1 or $GABA_AR$ γ2 and surface Flag-Shisa7 in cultured hippocampal neurons, Flag-Shisa7 were transfected into the neurons at DIV15 using Lipofectamine 3000. 24 hrs after transfection, coverslips were fixed in fixation buffer for 15 min

followed by washing and the incubation with anti-$GABA_AR$ α1 or $GABA_AR$ γ2 and anti-Flag antibodies with 5% NGS in 1x PBS for 5 hrs at RT. After washing, cells on coverslips were incubated with an anti-gephyrin antibody in 1x PBS with 3% NGS and 0.2 % Triton X-100 for overnight. After overnight incubation, coverslips were washed 5 min in 1x PBS for three times and then were incubated in secondary antibodies for 1 hr at RT followed by 3x 5-min washes and mounting.

For labeling of surface GluA1, surface Flag-Shisa7, and Homer1 in cultured Shisa7 KO hippocampal neurons, Flag-Shisa7 were transfected into the neurons at DIV15 using Lipofectamine 3000. 24 hrs after transfection, coverslips were fixed in fixation buffer for 15 min followed by washing and the incubation with anti-GluA1 and Flag antibodies with 5% NGS in 1x PBS for 5 hrs at RT. After washing, cells were incubated with an anti-Homer1 antibody in 1x PBS with 3% NGS and 0.2 % Triton X-100 for overnight to label Homer1 at 4°C. After overnight incubation, coverslips were washed 5 min in 1x PBS for three times and then were incubated in secondary antibodies for 1 hr at RT followed by 3x 5-min washes and mounting.

For the colocalization of endogenous Shisa7 and gephyrin under Airyscan, cultured hippocampal neurons were fixed in fixation buffer for 15 min at DIV16. After washing, cells on coverslips were incubated with anti-Shisa7 and gephyrin antibodies in 1x PBS with 3% NGS and 0.2 % Triton X-100 for overnight at 4°C. The coverslips were washed 5 min in 1x PBS for three times and then were incubated in anti-mouse Alexa conjugated 488, and anti-rabbit Alexa conjugated 555 secondary antibodies for 1 hr at RT followed by 3x 5-min washes and mounted using ProLong glass antifade mountant (Invitrogen, P36980).

For the colocalization of endogenous Shisa7 and surface $GABA_AR$ γ2 under Airyscan and STED, cultured hippocampal neurons were fixed in fixation buffer for 15 min at DIV16 followed by washing and the incubation of an anti-$GABA_AR$ γ2 antibody for 5 hrs at RT. After washing, cells on coverslips were incubated with an anti-Shisa7 monoclonal antibody in 1x PBS with 3% NGS and 0.2 % Triton X-100 for overnight. The coverslips were washed 5 min in 1x PBS for three times and then were incubated in Alexa conjugated 594 AffiniPure goat anti-mouse (for endogenous Shisa7, Jackson ImmunoResearch, 115-585-003) and Atto 647N goat anti-Rabbit (for sγ2, Active Motif, #15048) secondary antibodies for 1 hr at RT followed by 3x 5-min washes and mounted using ProLong glass antifade mountant.

Cell adhesion assay.
The cell aggregation assay was performed as described previously with minor modifications (*42, 43*). Briefly, HEK cells grown to a density of 1 x 10^5 cells/mL were transfected with total 6 µg of GFP, Shisa7-IRES-GFP, mCherry or $\alpha1\beta2\gamma2$/mCherry. 48-hr after transfection, trypsinized HEK cells were mixed at a 1:1 ratio and rotated for 2 hrs at RT. Cells were then placed in non-coated glass bottom dish (WillCo-Dish, GWSt-3512, #1.5, 12 mm) and subsequently incubated for an additional 30 min at RT. Live cells were imaged using a Zeiss 880 confocal microscope with a 10x objective. Cell adhesion index was analyzed using ImageJ, measuring the percentage of adhesion cells forming complexes of two or more cells relative to the total cell numbers.

Image acquisition and analysis
For immunostaining, images were acquired on a Zeiss LSM 880 laser scanning confocal microscope using a 63x oil objective (1.4 numerical aperture). Multiple *z* sections (7 optical slices) were acquired at 0.39 µm intervals. Images were captured using a 1024 x 1024 pixel screen for both of HEK and neuronal cells, and gains for fluorophores were set between 700 and 800 while multiple z sections of secondary apical dendrites were collected at 1.0–1.5 µm intervals with a

512 x 128 pixel screen for the co-localization experiments. Pinhole was set to 1 airy unit for all experiments. Scan speed function was set to 8 and the mean of 4 lines with double directions was applied. Laser power, digital gain, and offset settings were made all identical in each experiment by using the “reuse” function in LSM software.

For quantitative analysis of immunostaining in HEK cells and in neurons, maximal projection images were created with ZEN software (Zeiss) from 7 serial optical sections. A dendritic outline was drawn to cover 20-30 μm in length (representing a surface area of 850-1,000 pixels). The integrated fluorescent intensity of the target protein was calculated from one segment of the dendrite positive for Flag- or HA- Shisa7 using ImageJ (v1.5s). The choice of HA or Flag tag was based on antibody compatibility. A similar procedure was performed for quantitation of the fluorescence signal from surface and total $GABA_AR$ α2, β2 or β3 in HEK cells or surface/total $GABA_AR$ α1, α2 and γ2 subunits in neurons. Background was subtracted by using the “subtract background” function and the background level was held identical for all cells within each experiment. The region of interest (ROI) in cultured neurons was defined along a segment of the dendrite 20-30μm according to the fluorescence signal distinguished from the background. The ROI in HEK cells was defined along the cell body according to the fluorescence signal distinguished from the background. Average values of fluorescence intensities in ROI (the total fluorescent intensity divided by the total area of a dendritic segment) were calculated by ImageJ. For co-localization analysis in cultured hippocampal neurons, secondary dendritic segments were chosen as ROI. Flag- or HA- Shisa7, and gephyrin puncta were thresholded and confirmed visually to select appropriate clusters following a minimal size cut-off, which included all recognizable clusters. The co-localization percentage was quantified by the measurement of HA-Shisa7-positive gephyrin puncta divided by total number of thresholded gephyrin puncta or gephyrin-positive HA-Shisa7 puncta divided by total HA-Shisa7 puncta numbers. 15-40 dendrites were analyzed from approximately 10-20 neurons.

For super-resolution imaging of co-localization using the Zeiss Airyscan, mounted coverslips were imaged using a 63X objective with a Zeiss LSM 880 with Airyscan at the Microscopy and Imaging Core, NICHD, NIH. The Orthographic views with x, y and z planes were exported in ZEN software. The quantification analysis of overlap coefficient and correlation (R) between sFlag-Shisa7 and sα2 in HEK cells, Shisa7 and gephyrin, or Shisa7 and sγ2 in hippocampal neurons was measured in ZEN plugin Co-localization (Zeiss).

For super-resolution imaging of co-localization using the Stimulated emission depletion (STED) microscope, STED images from HEK cells and hippocampal neurons were acquired with Leica TCS SP8 STED 3x microscope that is equipped with a 100x 1.4 NA HC PL APO CS2 oil immersion objective and operated with the LAS-X imaging software. Excitation was with a tunable white light laser and emission was detected with hybrid detectors. In time-gated STED mode, Alexa 594 and Atto 647N were sequentially excited at 580 and 640 nm, respectively, with the 775 nm STED depletion beam, and their fluorescence collected at 585-635 nm and 645-760 nm, respectively. The STED resolution in our conditions was ~60 nm on the microscopic X- and y axis (parallel to the coverslip), and ~150-200 nm on the microscopic Z axis. STED images were deconvolved using Huygens software (Scientific Volume Imaging). For co-localization quantification, STED images were pre-processed with subtraction of a median filter-processed image and background, and then two images were proceeded to the ImageJ plugin JAcoP. Manders’ co-localization coefficient was chosen since it is sensitive to noise and background; true structural pixels were identified by applying a threshold to the images; all pixels with intensities above this threshold were considered to be an object. The threshold value was defined manually after visual inspection as previously described (*44*). The coefficient ratio of transfected Flag-

Shisa7 in HEK cells or endogenous Shisa7 in neurons with $GABA_AR$ subunits was quantitated by calculating sα2-positive sFlag-Shisa7 v.s. total sFlag-Shisa7 puncta in HEK cells, or sγ2-positive Shisa7 v.s. total Shisa7 puncta in cultured hippocampal neurons, using Manders' co-localization coefficient analysis in ImageJ.

Coimmunoprecipitation (co-IP) and Western blot

After transfection for 48 hrs, HEK cells were rinsed once with ice-cold 1x PBS and collected in a centrifuge tube. After centrifugation at 800 g for 5 min, the pellet was suspended in fresh ice-cold IP lysis buffer containing 25 mM Tris pH 7.5, 1% Triton X-100, 150 mM NaCl, 5% glycerol, 1 mM EDTA and protease inhibitor cocktail (Roche, 05892791001), and underwent constant shaking for 60 min on ice. The insoluble debris was removed by centrifugation at 12,000 g for 15 min. The soluble supernatant was then separated into input and IP lysates. An equal amount of the IP lysate was incubated with pre-washed anti-Flag M2 antibody conjugated to affinity agarose gel (Sigma-Aldrich, A2220, mouse) for overnight at 4°C while rotating. After centrifuging 5 min at 800 g, the gel beads were collected and washed 3 times with ice-cold lysis buffer. The bound proteins were finally eluted with 2x SDS loading buffer with β-mercaptoethanol, and denatured at 37°C for 10 min. The samples were subjected to SDS-PAGE and Western blot with indicated antibodies.

For co-IP in brain tissues, the hippocampi from 6-8-week-old Shisa7 WT and KO mice were dissected and homogenized in the pre-chilled 1x sucrose buffer (0.32 M Sucrose, 1 mM EDTA, 5 mM Tris, pH 7.4, protease inhibitor cocktail). After centrifugation at 800 g for 5 min, the supernatant was collected and centrifuged at 12,000 g for 15 min. The pellet was then resuspended in the pre-chilled lysis buffer (Tris-HCl 20 mM, NaCl 150 mM, 2% TritonX-100, EDTA, 5 mM with protease inhibitor cocktail and phosphatase inhibitor), followed by an incubation on ice for 1 hr. The lysates were then centrifuged at 12,000 g for 15 min and the supernatant was collected and incubated with primary antibody overnight. The anti- Shisa7, GluA1, $GABA_AR$ α1, $GABA_AR$ α2 antibodies or a control IgG (5-8 μg/ml) was used for co-IP. Hippocampal lysates were separately incubated with the above antibodies overnight at 4°C, followed by an incubation with 60 μl protein G or A dynabeads (ThermoFisher, 10007D for rabbit antibody or 10006D for guinea pig antibody) for 2 hrs at 4°C. After washing the beads with the same lysis buffer 4 times, the bound proteins were eluted, and the eluted proteins were denatured at 37°C for 10 min and subjected to SDS-PAGE and Western blot with indicated antibodies.

Hippocampal synaptosomal extraction was performed as described (*45*). Briefly, the hippocampi from 6-8-week-old Shisa7 WT and KO mice were dissected and homogenized in the pre-chilled 1x sucrose buffer. After centrifugation at 800 g for 5 min., the supernatant was centrifuged at 12,000 g to collect the pellet. The pellet was then resuspended in pre-chilled lysis buffer. After 12,000 g centrifugation for 15 min, the supernatant was slowly pipetted in each tube containing Percoll gradients (top to bottom: 3%, 10%, 15% and 23% Percoll in 1x sucrose buffer; Percoll: GE Healthcare, 17-0891-01) which was prepared less than 20 hrs before. The balanced tubes were then centrifuged at 31,000 g at 4°C in a Beckman JA-20 rotor for 6 min. The synaptosomal fractions were collected from the layer between 15% and 23% and diluted to ~30 ml with ice-cold 1x sucrose buffer in 50 ml polycarbonate centrifuge tubes. The balanced tubes were then centrifuged at 20,000 g in the Beckman JA-20 rotor for 30 min at 4°C. The pellets containing crude synaptosomal fractions were centrifuged again at 20,000 g for 30 min to remove the rest of sucrose buffer. The isolation of soluble and insoluble postsynaptic fractions was performed as described before with minor modifications (*46*). Briefly, crude synaptosomal fractions were treated with 0.5% Triton X-100 followed by centrifugation at 32,000 g for 30 min. The insoluble pellets were recovered as postsynaptic fractions.

Hippocampal total lysates and postsynaptic fractions from WT and KO hippocampi were quantified with the standard BCA method. An equal amount of loading samples was mixed with an equal volume of 2x SDS loading buffer and incubated for 5 min at 37°C, and then loaded onto pre-casted 12% SDS-PAGE gels (BioRad, 4561044). The proteins were transferred onto PVDF membranes, blocked, and incubated with indicated primary antibodies overnight at 4°C. The PVDF membranes were then washed three times with 0.1% TBST and incubated with HRP-conjugated secondary antibodies for 1 hr at RT. Protein was detected using the standard enhanced chemiluminescence (ECL) method and the bands were acquired and quantified with digital imager (Li-COR Odyssey).

Electrophysiology

Electrophysiology in HEK cells. For sIPSC recordings in co-culture of hippocampal neurons and HEK cells, HEK cells were co-transfected with indicated $GABA_AR$ subunits and Neuroligin2/mCherry together with GFP or Shisa7/GFP in 6 cm dish. ~24 hrs after transfection, trypsinized HEK cells were plated with cultured hippocampal neurons (HEK cells: 8 x 10^3 cells/well; neurons: 1.5 x 10^5 cells/well) at DIV16. The HEK cells were utilized for electrophysiological recordings after 2-3 days of co-culture. At least 3-4 independent batches of co-cultures were used for each experiment. For GABA-induced whole-cell currents, HEK cells were co-transfected with indicated $GABA_AR$ subunits together with GFP or Shisa7/GFP plasmids by calcium phosphate transfection[3]. One day before transfection, HEK cells were plated on coverslips (12-mm) that were pretreated with poly-D-lysine in a 24-well plate. The cDNAs (α:β:γ2L:GFP = 1:1:3:1) were premixed with 2 M $CaCl_2$ and distilled water followed by gently mixing with 2 x HBS solution using a VWR mini vortexer for 5 s at 300 r.p.m. After 15 min incubation at RT, the mixture was gentle added in wells and incubated in 5% CO_2 at 37°C for 2 hrs. Coverslips were then transferred to cell media containing 10% CO_2 for 15 min to dissolve the DNA-Ca^{2+}-phosphate precipitates to lower cell toxicity. All recordings were performed in the time window of 40-72 hrs after transfection. Coverslips containing HEK cells were perfused continuously with an external solution (in mM): 140 NaCl, 5 KCl, 2 $CaCl_2$, 1 $MgCl_2$, 10 HEPES and 10 D-glucose, adjusted to pH 7.4 with NaOH. For sIPSCs of co-cultured cells and whole-cell currents in HEK cells, the internal solution contained (in mM): 70 CsMeSO4, 70 CsCl, 8 NaCl, 10 HEPES, 0.3 NaGTP, 4 Mg_2ATP and 0.3 EGTA, adjusted to pH 7.3 with CsOH. For whole cell currents in different combinations of $GABA_ARs$, saturated GABA (10 mM, Abcam, Ab120359, in aCSF) solution was sequentially applied for 2 s with an interval of 20 s. The I_{GABA} was calculated as the peak current evoked by GABA. For diazepam (DZ, Hospira)-mediated potentiation of GABA currents, GABA ($\alpha1\beta2\gamma2$ and $\alpha2\beta3\gamma2$: 3 μM; $\alpha1\beta3\gamma2$: 10 μM, non-saturating GABA at ~EC15-20 based on previous work (*47-53*)), GABA plus DZ (1 μM) and GABA were sequentially applied for 2 s, separated by a 28-s washing. The tip of mini-manifold was placed at approx. 100 µM away from the recorded cell. GFP/mCherry-positive HEK cells in co-cultured coverslips or GFP positive HEK cells were patched with 4-7 MΩ borosilicate glass pipettes. Spontaneous IPSCs (sIPSCs) in HEK cells in co-cultures and whole-cell currents in HEK cells were recorded at a holding potential −70 mV at RT and currents were filtered at 2 kHz and sampled at 10 kHz. Only cells with a stable series resistance of <25 MΩ throughout the recording period were included in the analysis.

For GABA dose-response curves in HEK cells, the HEK cells were transfected with indicated α2, β3, γ2 with pCAGGs-IRES-GFP or pCAGGs-Shisa7-IRES-GFP using calcium phosphate transfection at a ratio of 1:1:3:1, respectively. After 24-hr transfection, single GFP-positive cells were identified and used for electrophysiology. The extracellular solution contained the following (mM): 140 NaCl, 5 KCl, 10 HEPES, 10 glucose, 1 $MgCl_2$, 2 $CaCl_2$, pH = 7.4, Osmolarity = 295-300. The intracellular solution contained the following (in mM): 70 CsF, 75 CsCl, 2 $CaCl_2$, 2 $MgCl_2$, 10 HEPES, 10 EGTA, pH = 7.36, Osmolarity = 289. GABA (0.3-1000 μM) was delivered to

cells via an 8-channel barrel manifold (Automate Scientific) driven by a Valvelink 8.2 perfusion (Automate Scientific controller and an air pressure regulator controller box made in-house. A Master-8 pulse stimulator (A.M.P.I) was used to control the duration of drug delivery and wash intervals between drug. Briefly, each concentration was applied for 0.5 s, followed by a 10 s wash interval between each drug concentration. The wash duration was determined by applying a 1 mM saturating concentration of GABA repetitively and testing for changes in peak amplitude. To determine the GABA median effective concentration (EC_{50}), each concentration was normalized to the maximum response for a given cell. The log(agonist) vs. response--Variable slope (four parameters function) in Prism 8 was used to perform a Least squares regression and the $LogEC_{50}$ was used to compare for any differences between groups.

For outside-out patches, HEK cells were cultured in DMEM-FBS until approximately 90% confluent. One day prior to transfection, they were trypsinized and plated onto glass coverslips in 35 mm culture dishes at a density of 5 x 10^3 cells/dish. Each 35 mm dish of HEK cells were transfected with GFP, α, β and γ2L $GABA_AR$ plasmid DNAs in a ratio of 1:1:1:4. Shisa7 (400 ng), with the total plasmid DNA amount ~2 µg per dish. Transfection was performed via calcium phosphate transfection method for 5-20 hrs in a 3% CO_2 incubator and terminated by washing cells twice with divalent cation-free phosphate buffered saline. After washing, transfected HEK cells within DMEM-FBS medium were returned to the incubator. Cultures were used for patch clamp recording over the following 2-3 days. All recordings were performed at RT at a holding potential of -70 mV. Coverslips containing HEK cells were perfused continuously with an external solution (in mM): 140 NaCl, 5 KCl, 2 $CaCl_2$, 1 $MgCl_2$, 10 HEPES and 10 D-glucose, adjusted to pH 7.4 with NaOH. GFP positive HEK cells were patched with 5-8 MΩ borosilicate glass pipettes. The internal solution for outside-out patches was composed of (in mM): 145 CsCl, 2 $CaCl_2$, 2 $MgCl_2$, 10 HEPES and 10 EGTA, adjusted to pH 7.4 with CsOH. Outside-out patches pulled from transfected HEK cells were activated by brief (1 or 100 ms) exposure to GABA (5 mM) using a piezo-electric translator (Siskiyou). The speed of the solution exchange system was regularly calibrated by rapidly switching the solution perfusing an open patch pipette between standard extracellular solution and an extracellular solution that had been diluted by 50% with distilled water (*54*). Rapid application/removal of GABA (every 5 s) was performed using a Piezo-controlled fast application system (Siskiyou) with a double-barrel application pipette that enables solution exchange. Data were averaged from at least 6 to 8 traces and collected with a Multiclamp 700B amplifier, filtered at 2 kHz and digitized at 50 kHz.

Electrophysiology in neurons. Mouse pups at P14-16 after embryonic IUE were euthanized by decapitation. The brain was immediately placed in ice-cold cutting solution containing (in mM) 2.5 KCl, 0.5 $CaCl_2$, 7 $MgCl_2$, 1.25 NaH_2PO4, 25 $NaHCO_3$, 7 glucose, 1.3 ascorbic acid and 210 sucrose. The hippocampi were quickly dissected out on an ice-cold platform and immediately placed onto an ice-cold Agarose gel block (5% Agarose in 1x aCSF). The gel block was quickly glued on the cutting platform containing ice-cold cutting solution saturated with carbogen. 300µm transverse slices were cut and recovered at 32°C for 30 min. Slices were then maintained in aCSF (modified to contain 2.5 mM $CaCl_2$ and 1.3 mM $MgCl_2$) at RT for 60 min prior to recording. The slice was then transferred to a recording chamber that was mounted on an upright Olympus microscope (BX51WI). The slices in the recording chamber were continuously saturated with 95% O_2/5% CO_2. Fluorescence-positive neurons in hippocampal slices were identified by epifluorescence microscopy.

For mIPSC recording at RT, hippocampal slices prepared from mice electroporated with sgRNAs or from littermates of Shisa7 WT and KO mice were transferred to a submersion chamber on an upright Olympus microscope, and perfused with aCSF solution supplemented with TTX (0.5 µM),

DNQX (20 μM). For the effect of DZ on sIPSC in WT and KO hippocampal acute slices, DZ was applied for 6 min followed a wash-out. The frequency and amplitude of sIPSCs before and after DZ application were analyzed and potentiation of sIPSC frequency or amplitude was calculated as $Potentiation_{sIPSC} = I_{Dz}/\ I_{Baseline}$, where I is either the average frequency or amplitude of sIPSCs. For the effect of DZ on GABA-evoked $GABA_A$R-mediated whole-cell currents in cultured WT and KO hippocampal neurons, GABA (10 μM) (pilot studies indicated that GABA at lower concentration (3 μM) than 10 μM produced very diminished whole-cell currents in some of Shisa7 KO hippocampal neurons), GABA plus DZ (1 μM) and GABA were sequentially applied for 2 s, separated by a 28-s washing. The tip of mini-manifold for solution application was placed at ~ 100 μM away from the recorded cell.

All dual recordings involved simultaneous whole cell recordings from one GFP-positive neuron and a neighboring GFP-negative control neuron in the hippocampal CA1 region. Cells were recorded with 4-7 MΩ borosilicate glass pipettes at RT. The internal solution for IPSC contained (in mM) 70 $CsMeSO_4$, 70 CsCl, 8 NaCl, 10 HEPES, 0.3 NaGTP, 4 Mg_2ATP and 0.3 EGTA. The stimulus was adjusted to evoke a measurable, monosynaptic IPSC in both cells. IPSCs were measured at a holding potential of -70 mV in the presence of DNQX (20 μM). For AMPA and NMDA EPSCs, the internal solution contained (in mM) 135 $CsMeSO_4$, 8 NaCl, 10 HEPES, 0.3 NaGTP, 4 Mg_2ATP, 0.3 EGTA, 5 QX-314 and 0.1 Spermine. The stimulus was adjusted to evoke a measurable, monosynaptic EPSC in both cells. AMPA EPSCs were measured at a holding potential of -70 mV, and NMDA EPSCs were measured at +40 mV and at 100 ms after the stimulus, at which point the AMPA EPSC has completely decayed. In the scatter plots of IPSCs and EPSCs, each open circle represents one paired recording, and the closed circle represents the average of all paired recordings. Paired-pulse ratios (PPRs) of IPSCs and EPSCs were measured by giving two pulses at a 50-ms interval and taking the ratio of the two peaks of the IPSCs/EPSCs from an average of 30–50 sweeps. Series resistance was monitored and not compensated, and cells in which series resistance varied by 25% during a recording session were discarded. Synaptic responses were collected with a Multiclamp 700B amplifier (Axon Instruments, Foster City, CA, United States), filtered at 2 kHz and digitized at 10 kHz. All pharmacological reagents were purchased from Abcam, and other chemicals were purchased from Sigma.

For CCK/CB1-CA1 paired recordings, the hippocampal slices were prepared from P15-18 Shisa7 WT or KO littermate mice as indicated. Mice were anesthetized with isoflurane, and the brain was dissected in ice-cold sucrose substituted artificial cerebrospinal fluid (SSACSF) containing (in mM): 80 NaCl, 3.5 KCl, 1.25 NaH_2PO_4-H_2O, 25 $NaHCO_3$, 4.5 $MgCl_2$, 0.5 $CaCl_2$, 10 glucose, and 90 sucrose equilibrated with 95% O_2/5% CO_2. Transverse slices (300 μm thick) were cut using a VT-1200S vibratome (Leica Microsystems, Bannockburn, IL), allowed to recover in SSACSF at 33°C for 30 min, and then stored at RT in SSACSF until transferred to a recording chamber perfused at 3 ml/min at 30-32°C with aCSF containing (in mM) 130 NaCl, 3.5 KCl, 24 $NaHCO_3$, 1.25 NaH_2PO_4-H_2O, 10 glucose, 2.5 $CaCl_2$ and 1.5 $MgCl_2$ saturated with 95% O_2/5% CO_2 (pH 7.4 300-310 mOsm). Cells were visualized using a 40x objective and IR-DIC video microscopy (Zeiss Axioskop 2 FS Plus) and whole-cell recordings were made using a Multiclamp 700A amplifier (Molecular Devices, Sunnyvale, CA). Uncompensated series resistance (5–20 MΩ) was monitored throughout recordings via a -5 mV voltage step and recordings were discarded if changes >20% occurred in the postsynaptic cell. Recordings were acquired at 10-20 kHz (filtered at 4 kHz) using pClamp 9.0.1.07 and analyzed in Clampfit (Axon Instruments). CCK/CB1-CA1 pyramidal cell unitary IPSC (uIPSC) paired recordings were performed as previously described (*55*). Briefly, presynaptic interneurons were recorded in current clamp mode with electrodes (3-5 MΩ) filled with intracellular solution (ICS) containing (in mM): 130 K-gluconate, 10 HEPES, 0.6 EGTA, 2 $MgCl_2$, 2 Na_2ATP, 0.3 NaGTP and 0.5% biocytin (pH 7.3, 290-300 mOsm). Postsynaptic

pyramidal cells were recorded in voltage clamp mode with electrodes filled with ICS containing (in mM) 100 K-gluconate, 45 KCl, 3 $MgCl_2$, 2 Na_2ATP, 0.3 NaGTP, 10 HEPES, 0.6 EGTA (with or without 0.2% biocytin), for a calculated E_{Cl^-} of −27 mV. Unitary synaptic transmission was monitored by producing trains (25 pulses/50Hz) or pairs (50Hz) of action potentials in the presynaptic interneuron (held in current clamp around -70 mV) every 20s by giving 2 ms 1-2 nA current steps while holding the postsynaptic pyramidal cell at -70 mV in voltage clamp. Presynaptic cells were confirmed as CCK/CB1 interneurons by probing for depolarization induced suppression of inhibition (DSI) and/or asynchronous release. In addition, we examined post-hoc anatomical recoveries to sort presynaptic cells as perisomatic or dendrite targeting. uIPSC properties for each cell were analyzed using 10-20 consecutive events obtained shortly after establishing the postsynaptic whole cell configuration. Amplitudes reflect the average peak amplitude of all events including failures, while potency is the average peak amplitude excluding failures.

The weighted time constants of mIPSCs, uIPSCs and sIPSCs were calculated from the area under the peak-normalized currents, according to $\tau_{decay} = \frac{1}{I_{peak}} \int_{t_{peak}}^{t_0} I(t)dt$ (*56*), where t_0 was 100 ms (mIPSCs and CCKBC uIPSCs in neurons) or 200 ms (sIPSCs in co-cultures) after the peak and data analysis were done with Igor Pro 6.22A. To calculate deactivation or desensitization time constants of macroscopic currents in HEK cells evoked by 1ms or 100 ms GABA (5 mM) application, respectively, digitally averaged macroscopic recordings were fitted with double-exponential functions in Clampfit 10.2, and a weighted time constant was calculated from individual time constants (τ_{fast}, τ_{slow}) and their relative amplitude (A_{fast}, A_{slow}) as followings: $\tau_{weighted} = (\tau_{fast} \times A_{fast} + \tau_{slow} \times A_{slow})/(A_{fast} + A_{slow})$.

Post-embedding immunogold electron microscopy

Post-embedding immunogold labeling was based on established methods (*57, 58*) with slight modification. Briefly, adult littermates of WT and Shisa7 KO mice were deeply anesthetized with Isoflurane and perfused with 0.12 M PB containing 4% paraformaldehyde plus 0.2% glutaraldehyde (*59*). The brains were post-fixed for 2 hrs at 4°C and washed 3 times over 1 hr in 0.1 M PB with 4% glucose. Sagittal sections were cut at 350 µm and cryoprotected in glycerol (30 min each in 10%, 20% and 30% and 30% overnight). The sections were plunge-frozen in liquid propane at -184°C in a Leica EM CPC (Vienna, Austria), further processed and embedded in Lowicryl HM-20 resin using a Leica AFS freeze-substitution instrument and polymerized with UV light. For immunolabeling, thin sections (110-130 nm) were cut on a Leica EM UC7 Ultramicrotome and incubated in 0.1% sodium borohydride plus 50 mM glycine in 1x TBS plus 0.1% Triton X-100 (TBST), followed by 10% normal goat serum (NGS) in TBST. These sections were incubated in $GABA_AR$ α1 (1:100, MilliporeSigma, #06-868, Rabbit) or α2 (1:25, Synaptic Systems, 224103, Rabbit) antibodies in 1% NGS/TBST overnight, followed by immunogold labeling using whole antibodies bound to gold conjugates (5 nm, Ted Pella, Redding, CA, USA) in 1% NGS in TBST plus 0.5% polyethylene glycol (20,000 MW). Finally, sections were stained with Uranyl Acetate and Lead Citrate.

All electron microscopy images were taken from the hippocampal CA1 *stratum pyramidale* and proximal *stratum radiatum* with a JEOL JEM-2100 transmission electron microscope (Peabody, MA, USA) and Gatan Orius digital camera (Pleasanton, CA, USA). All images were stored in their original formats and final images for figures were prepared in Adobe Photoshop; levels and brightness/contrast of images were minimally adjusted evenly over the entire micrograph. The postsynaptic membrane-associated immunogold particles were defined as those less than 25 nm from the postsynaptic cell membrane, counted on scanned electron micrographs, and then analyzed using ImageJ (v1.51s) software. In figures and figure legends, the n was defined as the

number of immunogold positive PSDs/total analyzed PSDs or the number of immunogold positive synapses/total analyzed synapses. The immunogold density was defined as the total number of immunogold divided by the number of immunogold positive PSDs. The number of $GABA_AR$ subunit immunogold/synapse was calculated by the total number of immunogold divided by the number of immunogold positive synapses.

Animal behavior

Novel object interaction test (NOIT). The NOIT was performed as previously described with minor changes (*60*). Briefly, the NOIT was performed in an opaque plastic box (50 x 50 x 30 cm). Animals were habituated to the empty test apparatus for 10 min one day prior to the start of the test. In this test, the novel objects were two trapezoidal cylindrical cages with different colorful cover (A1 and A2) were placed in the apparatus 10 cm away from two adjacent corners of the box. Animals were allowed to travel in the test chamber for 10 min. The behavior was recorded using the digital video system, and the track was analyzed by AnyMaze software.

Social interaction test (SIT). The modified SIT compares the preference of a test subject for a sex and weight matched mouse against a trapezoidal cylindrical cage as previously described (*60*). Briefly, one empty novel object was placed into the center of test chamber as A3, and another trapezoidal cylindrical cage with mouse (Stranger) was put at the same position as NOIT. A randomly selected WT mouse of the same sex as the stranger mouse was placed into one assigned cage 5 mins before the subject mouse was placed into the test chamber. The stranger and subject mice were never housed together and thus were unfamiliar to each other. No social isolation was conducted on either mouse, the test duration was 10 min.

Marble bury test (MBT). The MBT was often used to model obsessive-compulsive behavior in rodents. The test chamber was an acrylic opaque cage, filled with ~5 cm (depth) of conventional mouse housing bedding. Twenty round dark-green colored glass marbles (diameter 2.0 cm) were distributed evenly in a 5 x 4 grid. The cage and bedding were used for a maximum of 4 male mice. Mice were gently patted on their heads before they were placed in the center of the cage. The latency to dig the bedding was recorded using a timer with a maximum allowed time of 3 min. After a total of 15 min, mice were removed from the test cage. The number of marbles left on top of the bedding was counted manually. Only marbles with more than half of its diameter visible were counted.

Elevated plus maze (EPM). The EPM test was a classical test used to measure anxiety-like behavior in rodents. Briefly, the platform was 50 cm above the floor, with all four arms measuring 10 cm (W) x 40 cm (L). The maze was constructed with black acrylic glass wall (30 cm) and white painted acrylic floor with mild crude surface. The EPM test was performed 30 min right after DZ (clinical grade DZ, Hospira, 1.5 mg/kg, i.p.) or vehicle administration. The animal was placed at the center zone with its head toward the close arm. The behavior was recorded for 6 min using the digital video system and analyzed by AnyMaze software.

Loss of righting reflex (LORR). The loss and subsequent return of the righting reflex is an established behavioral paradigm to assess behavioral responsiveness in rodents (*61*). Specifically, with exposure to hypnotic doses of sedative drugs, mice that have been tipped onto their backs in a position of vulnerable dorsal recumbency, lose the protective response to flip back onto all four paws. The LORR assay was performed according to the procedures previously reported with minor changes (*62*). Briefly, animals were intraperitoneally injected with DZ (0, 3, 10, 30 or 50 mg/kg, Hospira) and immediately placed into a cage with mouse housing bedding. Since Hospira contains 10% ethanol, we also performed a parallel LORR test with DZ (50 mg/kg) without ethanol. LORR latency is the amount of time between DZ administration and LORR, and

LORR duration is defined as the amount of time between the loss and regaining of the righting reflex. Mice that failed to LORR within 30 min after administration of DZ were excluded but counted in the ratio of failure to LORR.

Locomotor activity. Animals were placed singly in a Plexiglas arena (50 x 50 x 30 cm) and allowed to habituate the cage for 15 min twice a day for two days. After the habituation, The WT and Shisa7 KO mice were intraperitoneally injected with 5 mg/kg DZ (without ethanol) administration 30 min before being placed in the activity cages. The total traveled distance was recorded using the digital video system for 30 min.

All of these above behavioral tests were conducted between 10:00-16:00 and were performed by a female technician.

Statistical analysis

For all biochemical, cell biological, ISH, EM and electrophysiological recordings, at least three independent experiments were performed (independent cultures, transfections or different mice). Statistical analysis was performed in GraphPad Prism 7.0 or OriginPro 8 software. Data sets were tested for normality and direct comparisons between two groups were made using two-tailed Student's *t* test (*t* test, for normally distributed data) or Mann-Whitney *U* tests (for non-normally distributed data sets) as indicated. Multiple group comparisons were made with one-way ANOVA analysis with post hoc Fisher's LSD test, or two-way ANOVA analysis with repeated measures for behavioral assays. The significance of the cumulative probability distributions was assessed with the Kolmogorov-Smirnov test. The statistical significance was defined as $*p < 0.05$, $**p < 0.01$, $***p < 0.001$ or $****p < 0.0001$, respectively. All data are presented as mean ± S.E.M.

Figure. S1

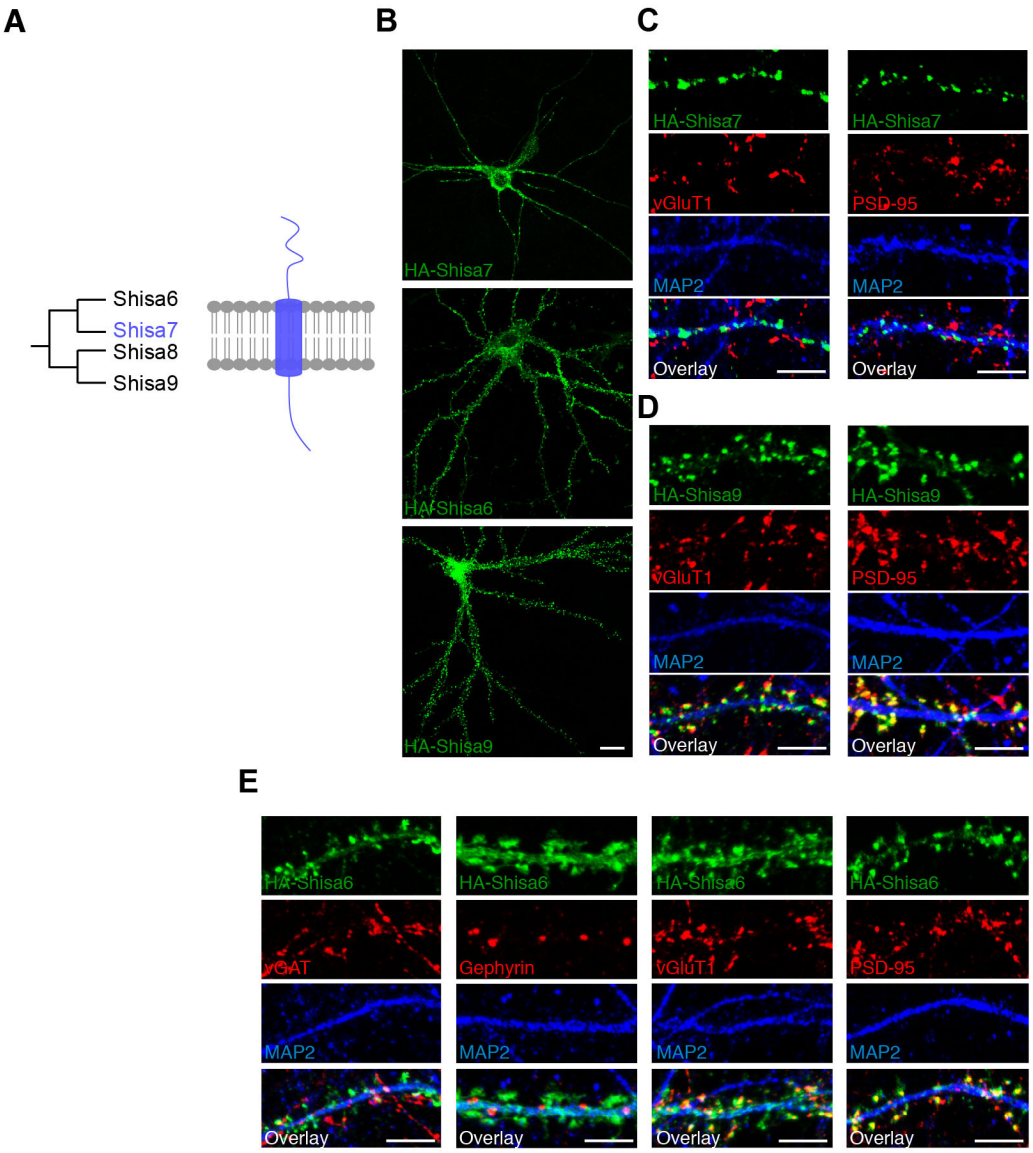

Fig. S1. Subcellular localization of Shisa6, 7 and 9 in hippocampal neurons. (A) Phylogenetic tree of Shisa6 to -9. Shisa proteins are single-passing transmembrane proteins. **(B)** Representative images at the low magnification of N-terminal HA-tagged Shisa6, 7 or 9 expressed in hippocampal cultured neurons. Tagged Shisa8 did not express well in hippocampal cultures under our experimental conditions. Scale bar, 10 μm. **(C)** Representative images at the high magnification showed that HA-Shisa7 did not co-localize with excitatory synaptic markers, vGluT1 or PSD-95. Scale bar, 10 μm. **(D)** Representative images at the high magnification showed that HA-Shisa9 co-localized with vGluT1 or PSD-95. Scale bar, 10 μm. **(E)** Representative images at the high magnification showed that HA-Shisa6 co-localized with vGluT1 or PSD-95, but not with inhibitory synaptic markers, vGAT or gephyrin. Scale bar, 10 μm.

Figure. S2

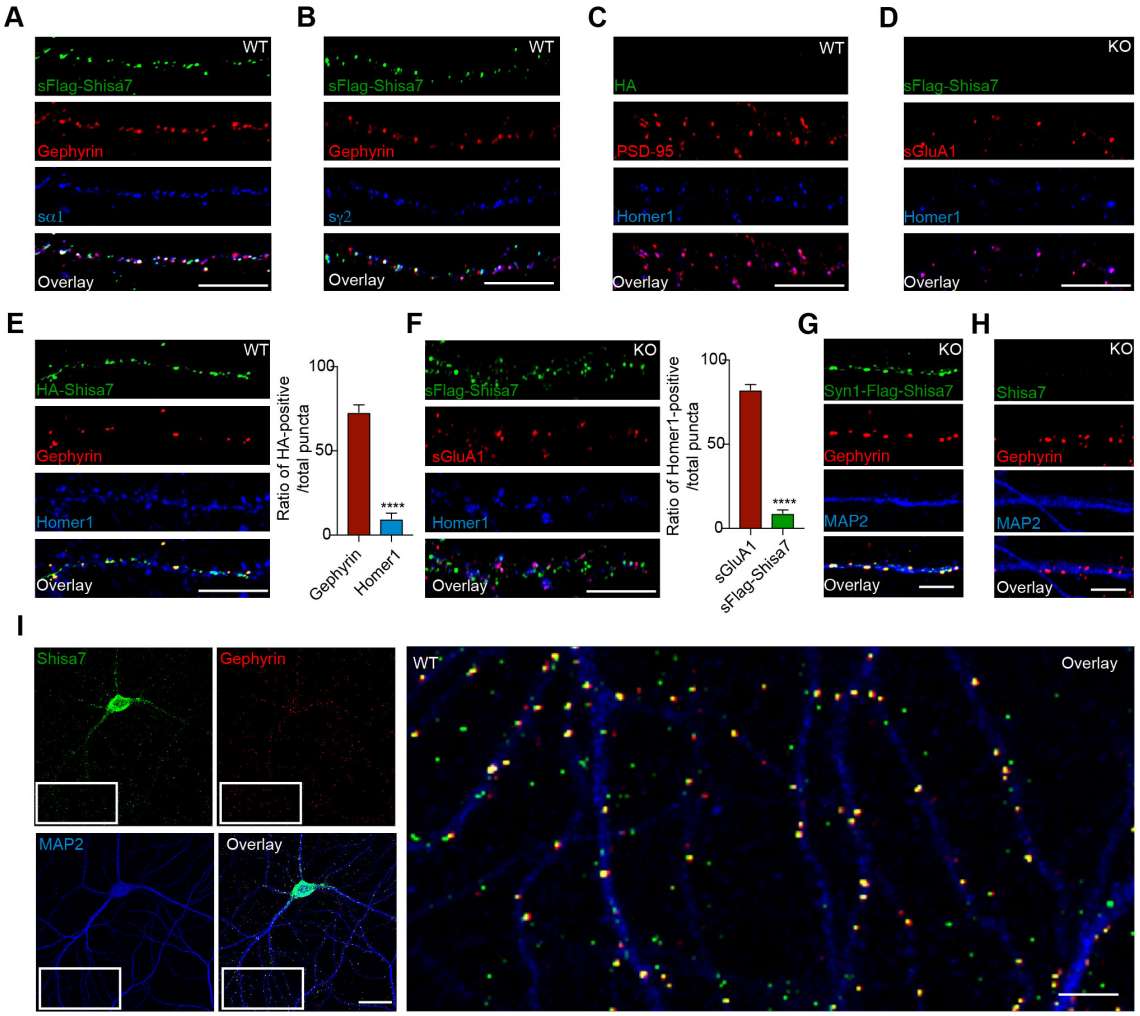

Fig. S2. Subcellular localization of expressed and endogenous Shisa7 in hippocampal neurons. (A-B) Shisa7 co-localized with $GABA_AR$ surface α1 (sα1) **(A)** and sγ2 **(B)** subunits in hippocampal neurons. Scale bar, 10 μm. **(C-D)** Homer1 co-localized with PSD-95 **(C)** and sGluA1 **(D)** in hippocampal cultured neurons [**C** (without expressing HA-Shisa7) was also a control for **E,** and **D** (without expressing Flag-Shisa7) was also a control for **F**]. Scale bar, 10 μm. **(E)** Homer1 did not co-localize with HA-Shisa7 or gephyrin in hippocampal cultured neurons (****$p < 0.0001$, *t* test). Scale bar, 10 μm. **(F)** Homer1 co-localized with sGluA1, but not with sFlag-Shisa7 in Shisa7 KO hippocampal cultured neurons transfected with Flag-Shisa7 (****$p < 0.0001$, *t* test.). Scale bar, 10 μm. **(G)** AAV-Syn1-Flag-Shisa7 expressing Flag-Shisa7 under the neuronal Synapsin1 promoter was transfected into Shisa7 KO hippocampal cultures. Flag-Shisa7 in Shisa7 KO cultured neurons co-localized with gephyrin. Scale bar, 5 μm. **(H)** Validation of the custom-made monoclonal antibody against endogenous Shisa7 (Mab7C10, which was suitable for immunocytochemical experiments) in cultured hippocampal neurons prepared from Shisa7 KO mice. No immunostaining was detected with Mab7C10 in Shisa7 KO neurons. Scale bar, 5 μm. **(I)** Representative images at the low (left) and high (right, boxed area at the left) magnification

showed that the vast majority of endogenous Shisa7 co-localized with gephyrin in cultured hippocampal neurons. Scale bar, top: 25 μm; bottom: 5 μm.

Figure. S3

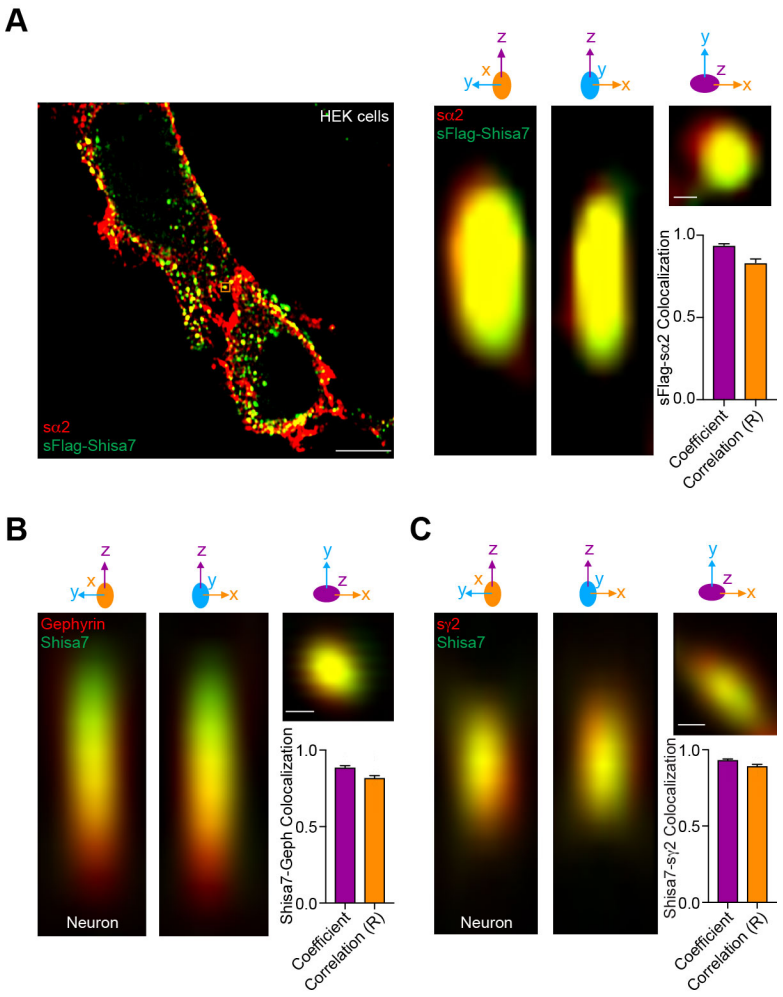

Fig. S3. Subcellular localization of expressed and endogenous Shisa7 in HEK cells and hippocampal neurons under Zeiss super-resolution Airyscan. (A) Representative Airyscan images showing single puncta co-labeling with sFlag-Shisa7 and sα2 (α2β3γ2) in HEK cells. "s" stands for surface. The quantitative analysis showed that sFlag-Shisa7 strongly co-localized with sα2. Data were quantified for the values of coefficient and correlation (R), n = 29 puncta. Scale bar: 5 μm (left), 100 nm (right). **(B-C)** Representative Airyscan images showing the puncta co-labeling with endogenous Shisa7 and gephyrin **(B)** or sγ2 **(C)** in cultured hippocampal neurons at DIV16. The quantitative analysis showed that Shisa7 strongly co-localized with gephyrin and sγ2. Data were analyzed based on the values of overlap coefficient and correlation (R), n = 30 puncta. Scale bar: 100 nm. Data are mean ± S.E.M.

Figure. S4

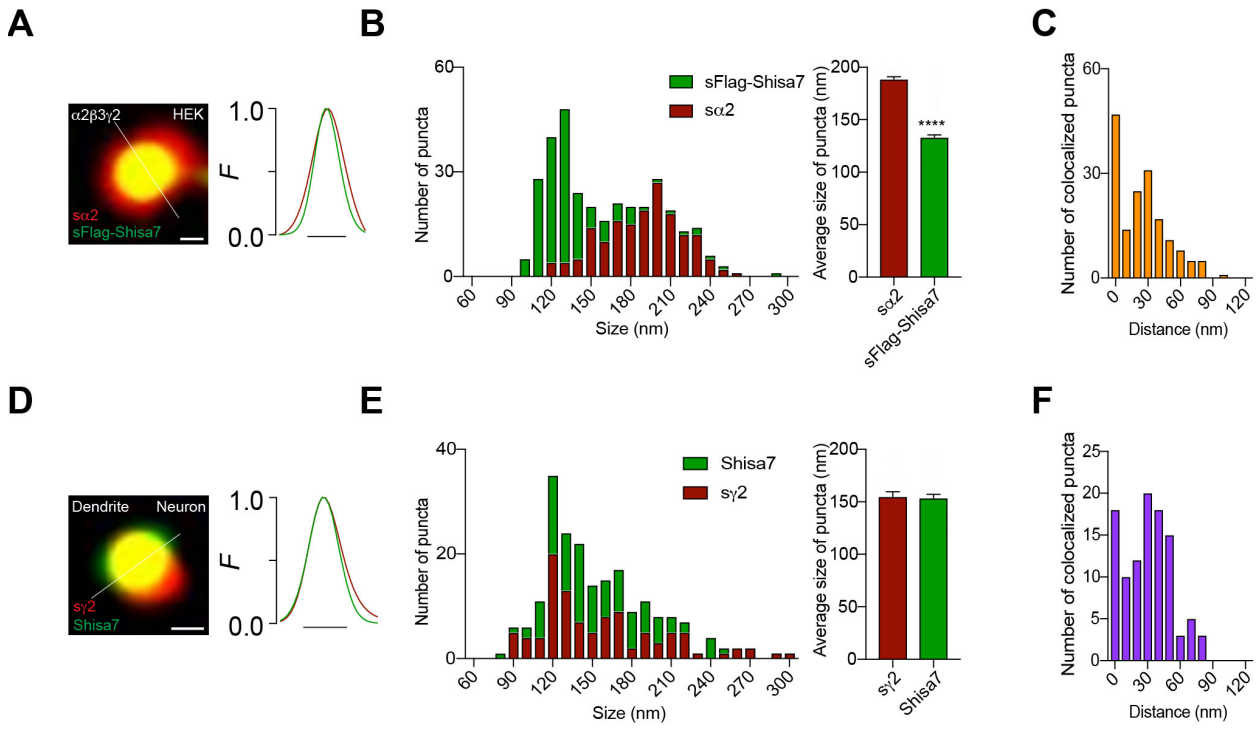

Fig. S4. Subcellular localization of expressed and endogenous Shisa7 in HEK cells and hippocampal neurons under STED. (A) The line profile of co-localized sFlag-Shisa7 (green) and sα2 (red) in HEK cells based on the image in Fig.1D (top). The fluorescence profile was measured across the grey line, *F* traces were also enlarged (lower). Line profiles were normalized to the peak value. Scale bar, 200 nm (top), 100 nm (bottom). (**B**) Distribution of puncta size showed that a single punctum of sFlag-Shisa7 was smaller than that of sα2 (n = 164 puncta, ****$p < 0.0001$, *t* test) in HEK cells. **(C)** Distribution of the center distance of co-localized sFlag-Shisa7 and sα2 (n = 164 puncta for each channel, quantitation analysis was based on the line profile of 164 ROIs). **(D)** The line profile of co-localized endogenous Shisa7 (green) and sγ2 (red) in cultured hippocampal neurons at DIV16 based on the image in Fig. 1D (bottom), *F* traces were also enlarged (lower). Scale bar, 100 nm (top), 50 nm (bottom). **(E)** Distribution of puncta size showed that a single punctum of endogenous Shisa7 was similar as that of sγ2 (n = 107 puncta, $p > 0.05$, *t* test) in neurons. **(F)** Distribution of the center distance of co-localized Shisa7 and sγ2 (n = 107 puncta for each channel, quantitation analysis was based on the line profile of 107 ROIs). Data are mean ± S.E.M.

Figure. S5

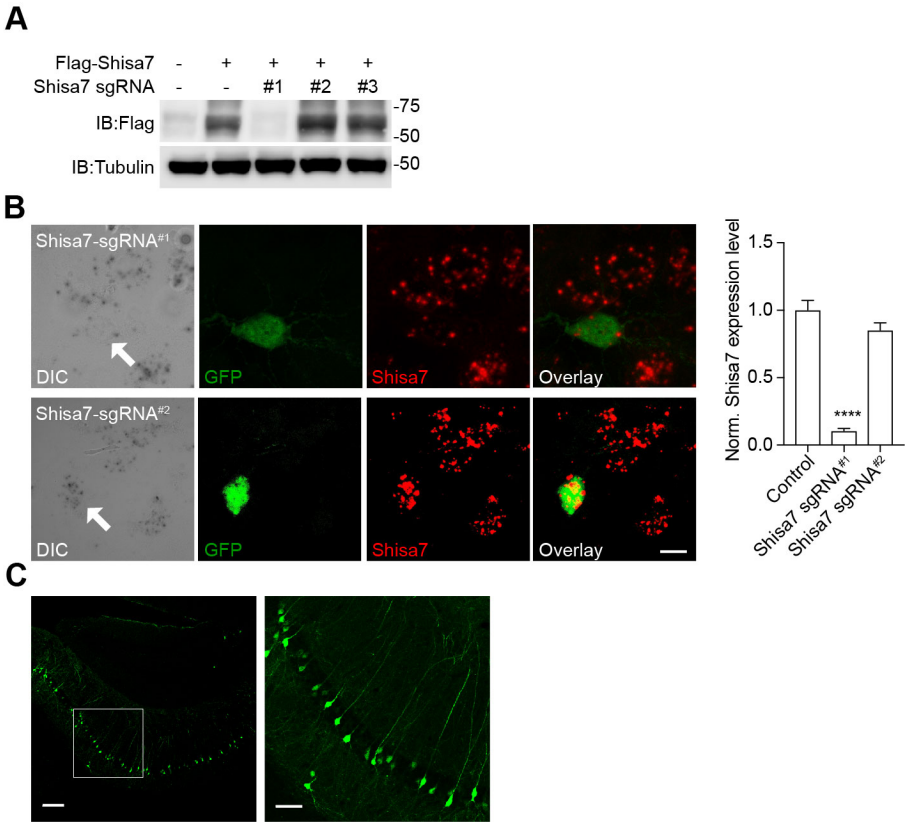

Fig. S5. Validation of Shisa7 sgRNAs. (A) Screening candidate sgRNAs against Shisa7 for CRISPR-Cas9 system mediated KO in HEK cells. **(B)** *in situ* hybridization (ISH) data showed that sgRNA$^{\#1}$, but not sgRNA$^{\#2}$, essentially eliminated *Shisa7* mRNA expression (in red) in cultured hippocampal neurons (Control: n = 12; sgRNA$^{\#1}$: n = 11; sgRNA$^{\#2}$: n = 10; normalized Shisa7 expression intensity: ****p < 0.0001, one-way ANOVA with post hoc Fisher's LSD test). Scale bar, 10 μm. **(C)** Representative image (left, low magnification; right, high magnification of the boxed area at the left) showing mosaic expression of GFP in CA1 neurons in an acute hippocampal slice prepared from mice underwent *in utero* electroporation of sgRNA$^{\#1}$ at E14.5. Scale bars, 100 mm (left) and 50 mm (right). Data are mean ± S.E.M.

Figure. S6

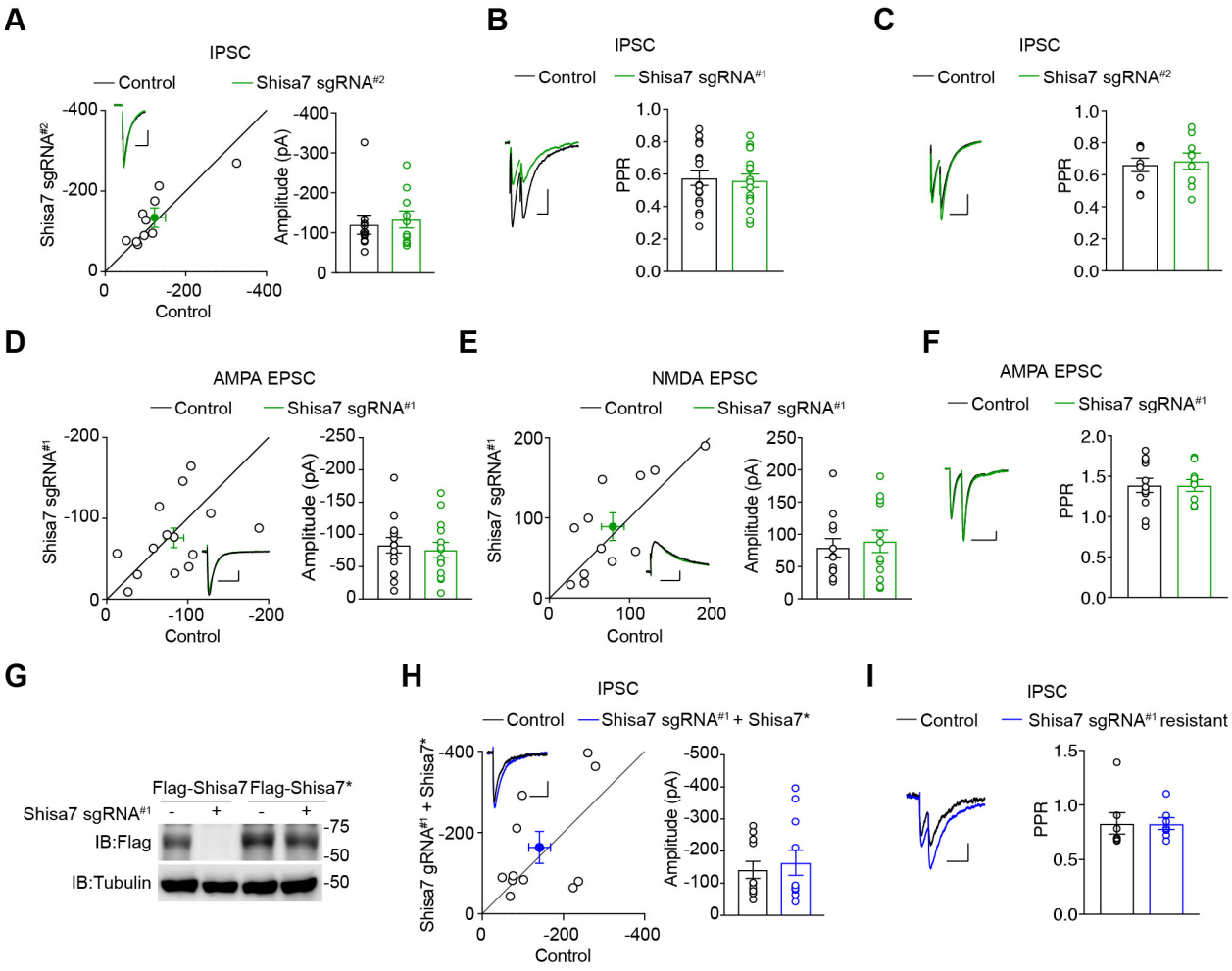

Fig. S6. Single-cell genetic deletion of Shisa7 does not change glutamatergic transmission. **(A)** Dual recording showed that Shisa7 sgRNA$^{\#2}$, a negative control to sgRNA$^{\#1}$, did not change IPSCs in CA1 pyramidal cells (sgRNA$^{\#2}$: n = 10, $p > 0.05$; paired *t* test). Scale bars, 20 pA and 1 s. **(B-C)** Single-cell genetic deletion of Shisa7 did not change the paired pulse ratio (PPR) of IPSCs (**B**, Control: n = 17; Shisa7 sgRNA$^{\#1}$: n = 17; $p > 0.05$, *t* test; **C**. Control: n = 9; Shisa7 sgRNA$^{\#2}$: n = 9; $p > 0.05$, *t* test). Scale bar, IPSC: 50 pA and 100 ms; **(D-E)** Single-cell genetic deletion of Shisa7 did not change AMPAR- **(D)** and NMDAR- **(E)** mediated EPSCs (AMPA: n = 14, $p = 0.58$, paired *t* test; NMDA: n = 12, $p > 0.05$, paired *t* test). The open circles represented all pair recordings, the solid circle showed the average of pair recordings. Scale bar, 20 pA and 100 ms. **(F)** Single-cell genetic deletion of Shisa7 did not change PPR of AMPA EPSCs (Control: n = 12; Shisa7 sgRNA$^{\#1}$: n = 10; $p > 0.05$, *t* test). EPSC: 20 pA and 100 ms. **(G)** sgRNA$^{\#1}$ failed to reduce the expression of sgRNA$^{\#1}$ resistant Shisa7 (Shisa7*) in HEK cells. Western blotting analysis showed that sgRNA$^{\#1}$ strongly reduced the expression of WT Flag-Shisa7, but not Flag-Shisa7*. **(H)** Co-expression of sgRNA$^{\#1}$ resistant plasmid, Shisa7*, with sgRNA$^{\#1}$ rescued IPSC deficits (n = 11, $p > 0.05$, paired *t* test) in CA1 pyramidal neurons. Scale bar, 50 pA and 100 ms. **(I)** Co-expression of Shisa7 gRNA$^{\#1}$ and Shisa7* did not change PPR of IPSCs (Control: n = 8; Shisa7*: n = 8, $p > 0.05$, *t* test). Scale bar, 50 pA and 100 ms. Data are mean ± S.E.M.

Figure. S7

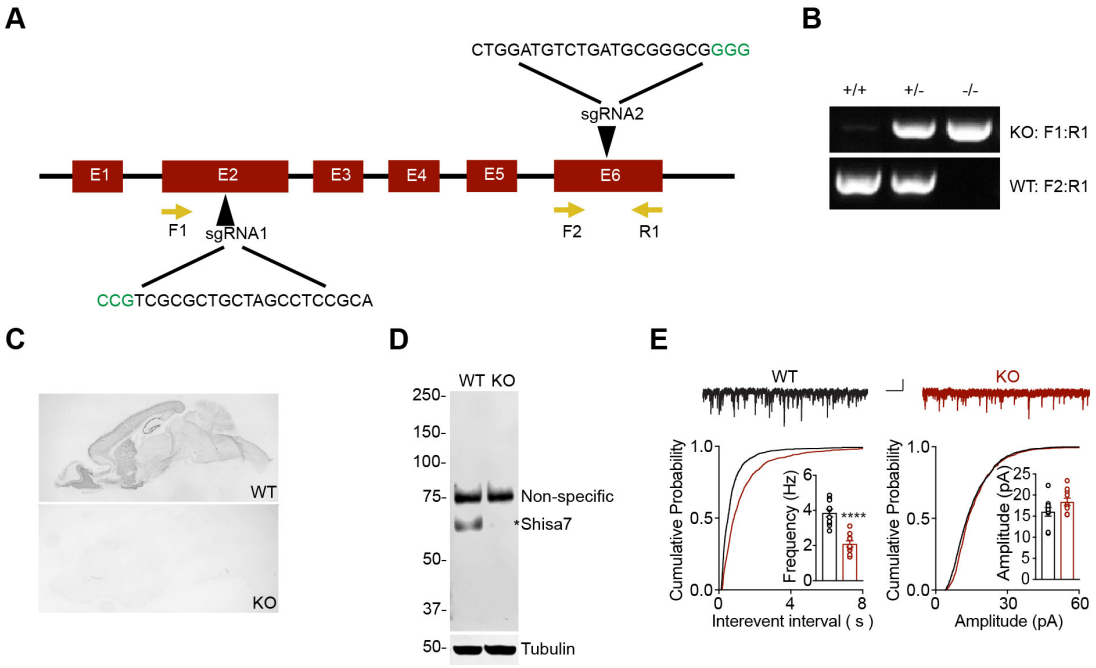

Fig. S7. Generation of Shisa7 germline knockout (KO) mice. (A) Schematic of the *Shisa7* gene and the sgRNA sequences located in Exon 2 and Exon 6 used to target the gene. The required PAMs (protospacer-adjacent motifs) are shown in green color. **(B)** Representative genotyping pattern of WT, Shisa7$^{+/-}$ and Shisa7$^{-/-}$ mice. Two pairs of PCR primers were designed to amplify the large deletion region of the Shisa7 transcript. **(C)** *In situ* hybridization of Shisa7 WT and KO mouse sagittal brain slices. **(D)** Western blotting of Shisa7 protein expression in hippocampal lysates prepared from WT and Shisa7 KO mice. The custom-made polyclonal rabbit antibody against sequence GTLARRPPFQRQGT (position 519–532 in Shisa7, which was suitable for immunoprecipitation and Western blot experiments) recognized Shisa7 in hippocampal lysates prepared from WT, but not Shisa7 KO, mice. * indicates the Shisa7 band. **(E)** Shisa7 KO reduced the frequency (***$p < 0.0001$, *t* test), but not the amplitude ($p > 0.05$, *t* test), of mIPSC (WT: n = 10; KO: n = 10). Scale bars, 10 pA and 1 s.

Figure. S8

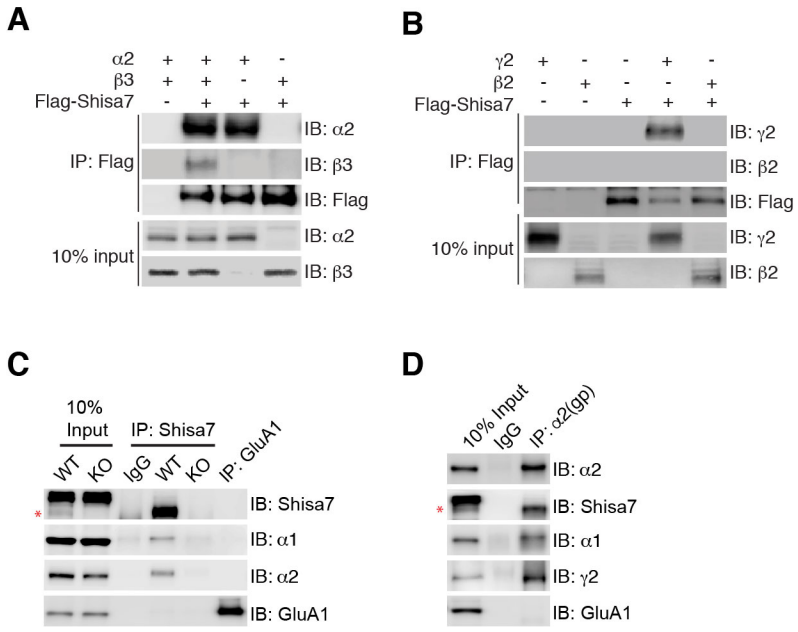

Fig. S8. $GABA_AR$ subunits were coimmunoprecipitated **with Shisa7 in HEK cells and in hippocampal lysates. (A)** $GABA_AR$ α2, but not β3, subunits were coimmunoprecipitated with Flag-Shisa7 in HEK cells. **(B)** $GABA_AR$ γ2, but not β2, subunit was coimmunoprecipitated with Flag-Shisa7 in HEK cells. **(C)** $GABA_AR$ α1 or α2 subunits were coimmunoprecipitated with Shisa7 in hippocampal lysates prepared from WT, but not Shisa7 KOs. **(D)** Co-IP of $GABA_AR$ α2 subunit and Shisa7 in hippocampal lysates. Shisa7 was coimmunoprecipitated with an α2 antibody, but not with a control IgG. * indicates the Shisa7 band.

Figure. S9

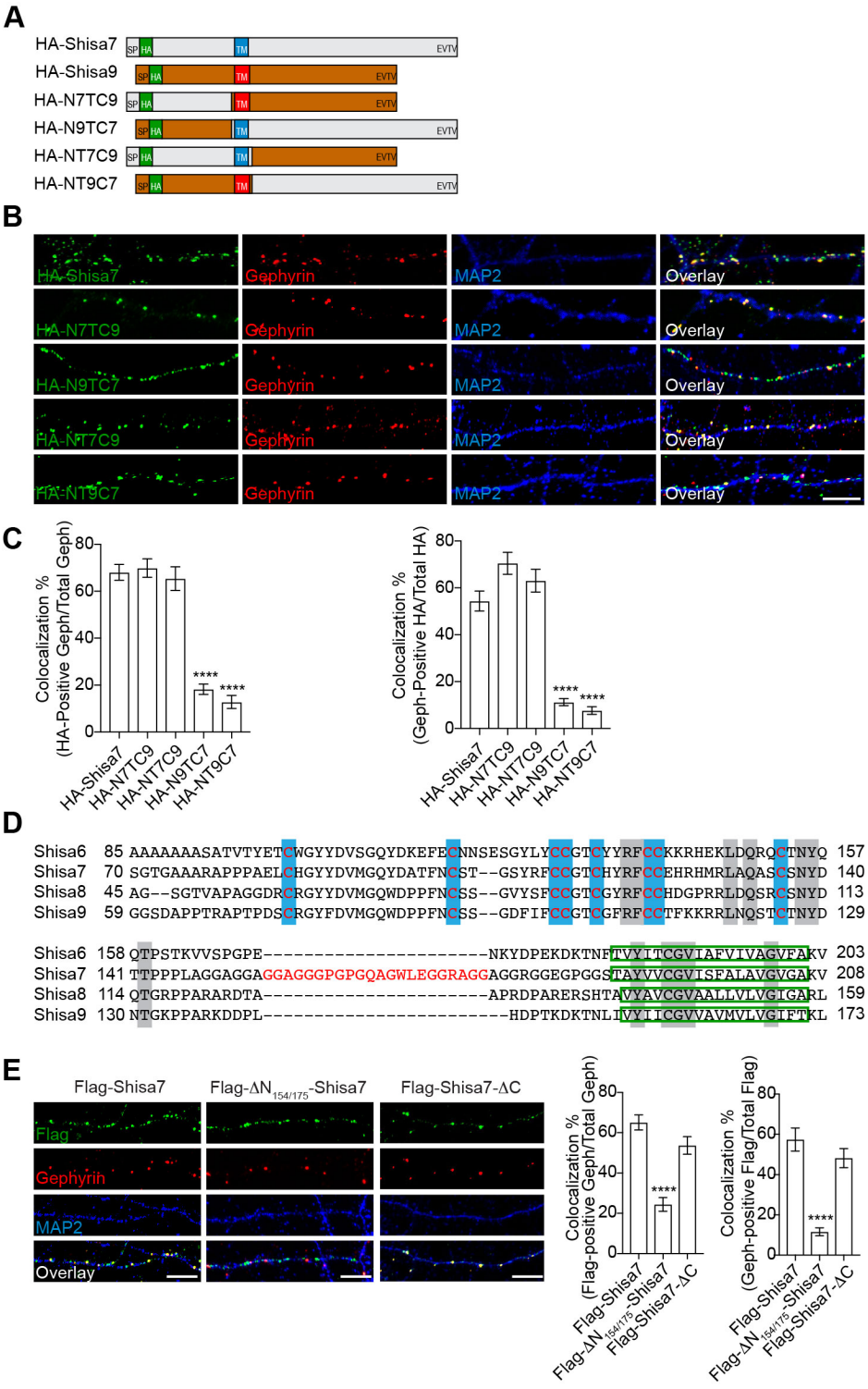

Fig. S9. Domain analysis of Shisa7 that mediates the co-localization with gephyrin. (A) Schematic of swap mutants of HA-Shisa7 and HA-Shisa9 (SP, signal peptide; TM, transmembrane domain). **(B)** Representative images showing the co-localization of HA-Shisa7 or

HA-Shisa7 and HA-Shisa9 swap mutants that contained the N-terminus of Shisa7 with gephyrin in cultured hippocampal neurons. Scale bar, 10 μm. **(C)** Bar graphs showing the percentage of co-localization of HA-positive gephyrin to total gephyrin (Shisa7: n = 19; HA-N7TC9: n = 12; HA-NT7C9: n = 11; HA-N9TC7: n = 17; HA-NT9C7: n = 14; ****$p < 0.0001$, one-way ANOVA analysis with post hoc Fisher's LSD test) and the percentage of co-localization of gephyrin-positive HA to total HA (Shisa7: n = 19; HA-N7TC9: n = 12; HA-NT7C9: n = 11; HA-N9TC7: n = 17; HA-NT9C7: n = 14; ****$p < 0.0001$, one-way ANOVA analysis with post hoc Fisher's LSD test). **(D)** Protein sequence alignment of a part of N-terminus and the transmembrane domain of mouse Shisa6 to -9. Positions of conserved cysteines in the cysteine-knot motif were indicated in blue. Highly conserved amino acids were highlighted in gray. Predicted transmembrane regions were marked by green rectangle. A stretch of amino acids (22 amino acids, GRID) between the conserved cysteine-knot motif and the transmembrane domain in Shisa7 was highlighted in red. **(E)** The majority of Flag-Shisa7 or Flag-Shisa7ΔC, but not Flag-$\Delta N_{154/175}$-Shisa7, co-localized with gephyrin in hippocampal neuronal cultures (Flag-Shisa7: n = 31; Flag-$\Delta N_{154/175}$-Shisa7: n = 18; Flag-Shisa7ΔC: n = 23; ****$p < 0.0001$, one-way ANOVA with post hoc Fisher's LSD test). Scale bar, 10 μm. Data are mean ± S.E.M.

Figure. S10

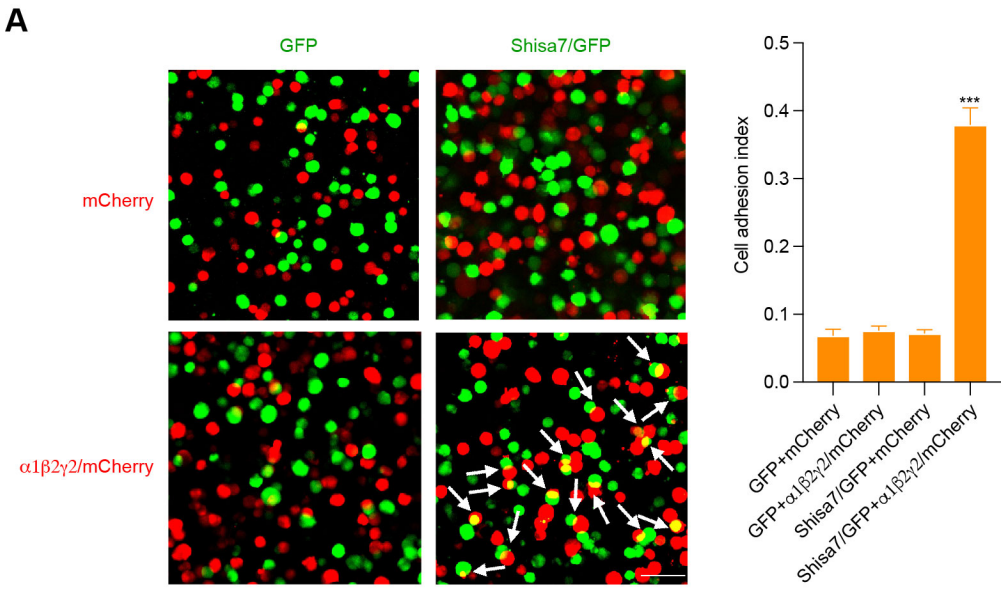

Fig. S10. A cell-based adhesion assay suggests a direct interaction between Shisa7 and GABA$_A$Rs. The representative images showing the cell adhesion between Shisa7 and GABA$_A$R $\alpha1\beta2\gamma2$ complex. Arrows indicated adhesion between cells expressing Shisa7-IRES-GFP and cells expressing $\alpha1\beta2\gamma2$ plus mCherry. The quantification of cell adhesion index showed a strong adhesion between cells expressing Shisa7 and cells expressing $\alpha1\beta2\gamma2$, but not in other conditions (n = 11 for each group, ***$p < 0.001$, One-way ANOVA with post hoc Fisher's LSD test). Scale bar, 50 μm. Data are mean ± S.E.M.

Figure. S11

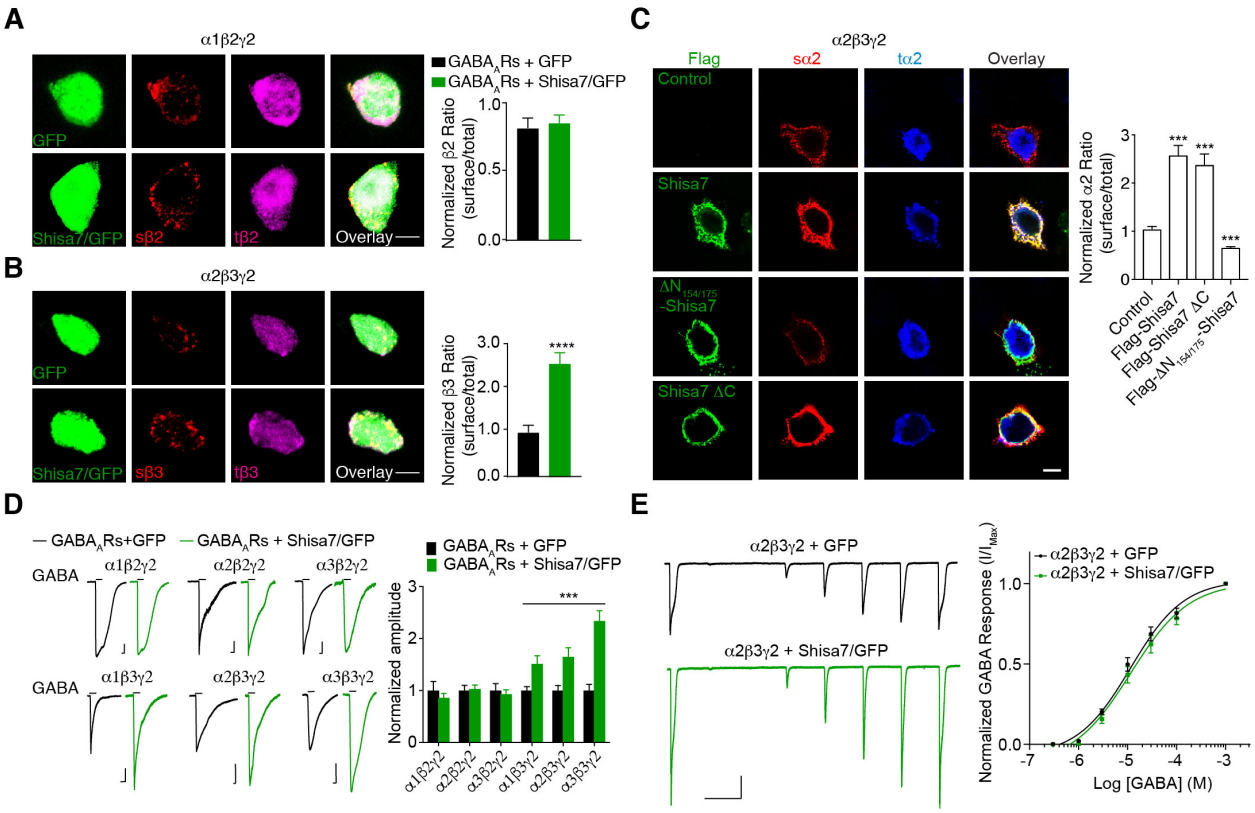

Fig. S11. Shisa7 increases surface expression of GABA$_A$R subunits in HEK cells. (A) HEK cells were co-transfected with Shisa7-IRES-GFP or GFP together with GABA$_A$R α1, β2 and γ2. Immunostaining of surface and total β2 showed that Shisa7 did not change the ratio of surface β2 (sβ2) / total β2 (tβ2) at the HEK cell surface. Bar graphs showed normalized ratio of sβ2 and tβ2 (GFP: n = 25; Shisa7/GFP: n = 25; p = 0.68, t test). Scale bar, 20 μm. **(B)** HEK cells were co-transfected with Shisa7-IRES-GFP or GFP together with GABA$_A$R α2, β3 and γ2. Immunostaining of surface and total β3 showed that Shisa7 increased the ratio of surface β3 (sβ3) / total β3 (tβ3) at the HEK cell surface. Bar graphs showed normalized ratio of sβ3 and tβ3 (GFP: n = 21; Shisa7/GFP: n = 19; ****p < 0.0001, t test). Scale bar, 20 μm. **(C)** HEK cells were co-transfected with GABA$_A$R α2, β3 and γ2, or together with Flag-Shisa7 or Flag-Shisa7 mutants. Representative images and bar graph showed that Flag-Shisa7 or Flag-Shisa7ΔC, but not Flag-ΔN$_{154/175}$-Shisa7, increased the surface/total ratio of α2 (Control: n = 15; Flag-Shisa7: n = 20; Flag-Shisa7 ΔC: n = 18; Flag-ΔN$_{154/175}$-Shisa7: n = 18; ****p < 0.0001, one-way ANOVA with post hoc Fisher's LSD test). Scale bar, 20 μm. **(D)** Shisa7 enhanced GABA-evoked whole-cell currents (GABA: 10 mM) in HEK cells expressing α1β3γ2, α2β3γ2 or α3β3γ2, but not α1β2γ2, α2β2γ2 or α3β2γ2 (α1β2γ2: GFP: n = 12; Shisa7/GFP: n = 17; α2β2γ2: GFP: n = 13; Shisa7/GFP: n = 13; α3β2γ2: GFP: n = 8; Shisa7/GFP: n = 8; α1β3γ2: GFP: n = 8; Shisa7/GFP: n = 8; α2β3γ2: GFP: n = 18; Shisa7/GFP: n = 21; α3β3γ2: GFP: n = 9; Shisa7/GFP: n = 9; ***p < 0.001, one-way ANOVA with post hoc Fisher's LSD test). Scale bar, 500 pA and 2 s. **(E)** Shisa7 did not significantly change GABA median effective concentration (EC$_{50}$) of α2β3γ2 GABA$_A$ receptors. A four-parameter, log agonist versus response nonlinear regression was used to obtain the EC$_{50}$ values and the LogEC$_{50}$ values were compared between both groups. Shisa7 did not significantly change GABA sensitivity for

$\alpha 2\beta 3\gamma 2$ $GABA_A$Rs (GFP: EC_{50} = 9.78 μM, n = 9; Shisa7/GFP*:* EC_{50} = 14.3 μM, n = 8, $p > 0.05$). Scale bar, 500 pA, 10 s. Data are mean ± S.E.M.

Figure. S12

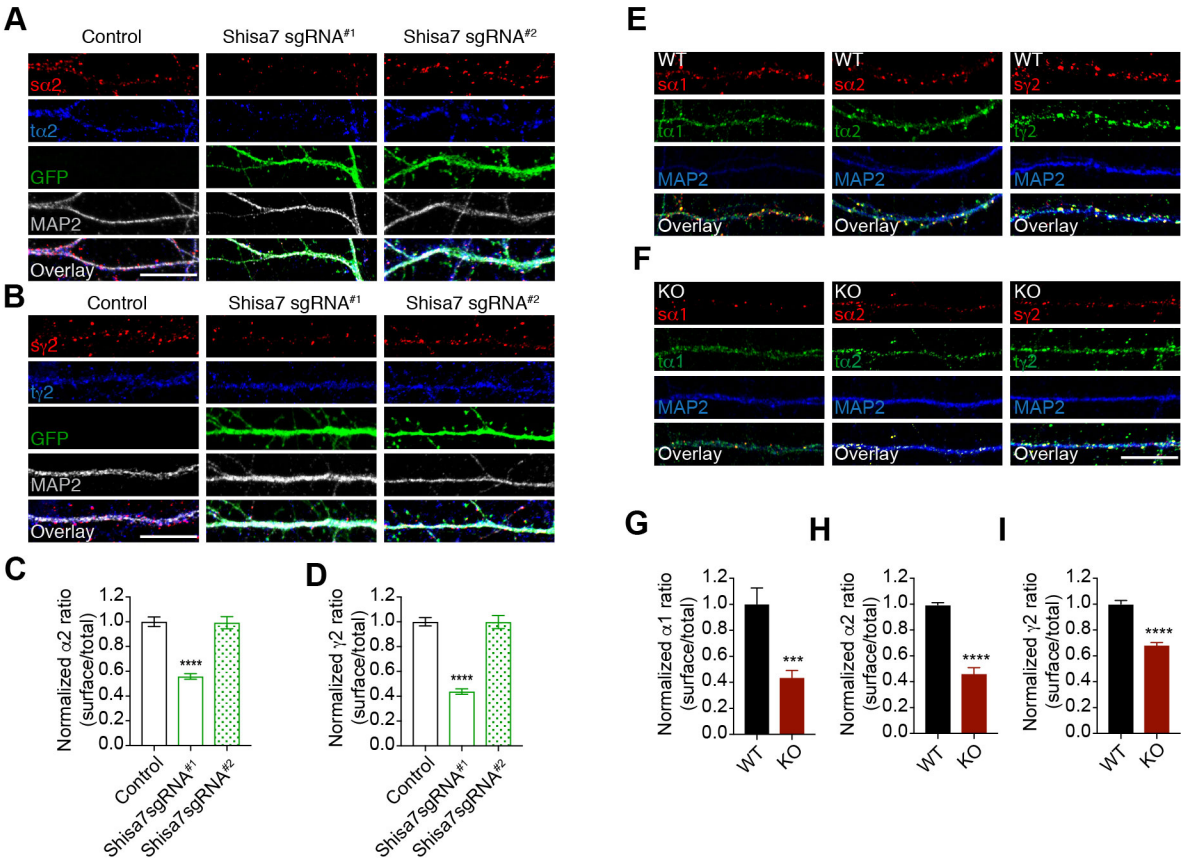

Fig. S12. Shisa7 is required for surface expression of GABA$_A$R subunits at neuronal surface. (A-D), Representative images showed that single-cell genetic deletion of Shisa7 reduced the surface expression levels (surface/total) of GABA$_A$R α2 **(A)** and γ2 **(B)** subunits in cultured hippocampal neurons at DIV15-16. Bar graphs in the bottom showed normalized ratio of surface (s) to total (t) α2 **(C)**, Control: n = 41; sgRNA$^{\#1}$: n = 21; sgRNA$^{\#2}$: n = 19; ****p < 0.0001, one-way ANOVA with post hoc Fisher's LSD test), and normalized ratio of surface to total γ2 **(D)**, Control: n = 27; sgRNA$^{\#1}$: n = 15; sgRNA$^{\#2}$: n = 12, ****p < 0.0001, one-way ANOVA with post hoc Fisher's LSD test). Scale bar, 10 μm. **(E-I),** Representative images of surface and total expression levels of GABA$_A$R α1, α2 and γ2 subunits in cultured hippocampal neurons at DIV15-16 prepared from E17.5-E18.5 WT **(E)** or Shisa7 KO **(F)** embryos. Bar graphs at the bottom showed normalized ratio of surface (s) to total (t) α1 (WT: n = 16; KO: n = 15, ***p < 0.001, t test), α2 (WT: n = 30; KO: n = 35, ****p < 0.0001, t test) and γ2 (WT: n = 35; KO: n = 42, ****p < 0.0001, t test), demonstrating that genetic deletion of Shisa7 significantly reduced surface expression of GABA$_A$R α1 **(G)**, α2 **(H)** and γ2 **(I)** subunits. Scale bar, 10 μm. Data are mean ± S.E.M.

Figure. S13

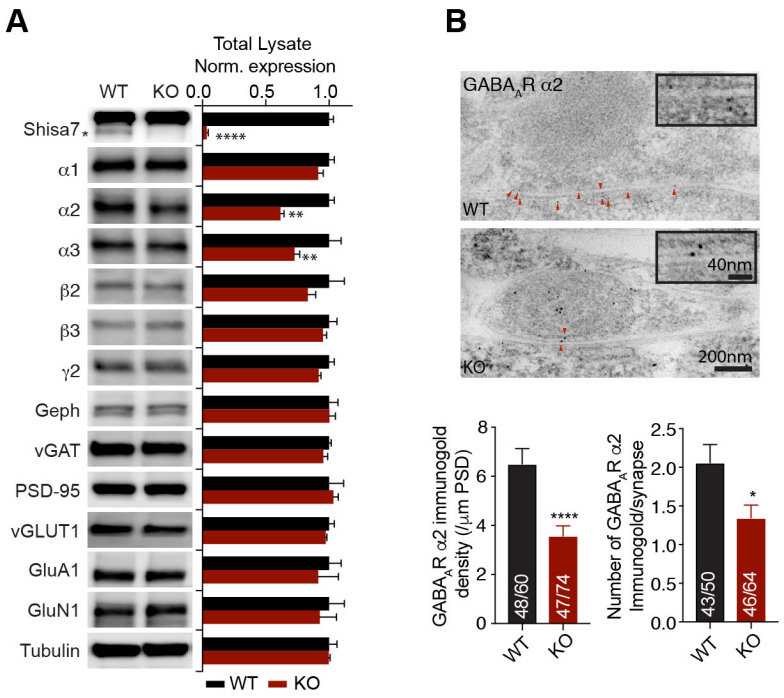

Fig. S13. Knockout of Shisa7 reduces the total protein expression levels of GABA$_A$R subunits and impairs synaptic abundance of the α2 subunit. (A) Shisa7 KO significantly reduced the total expression levels of α2 and α3 in mouse hippocampal lysates (Shisa7: ****p < 0.0001; α2: **p < 0.01; α3: **p < 0.001, one-way ANOVA with post hoc Fisher's LSD test). **(B)** Post-embedding immunogold labeling of GABA$_A$R α2 subunit in WT and Shisa7 KO hippocampal CA1 somatic region. Quantifications of the α2 immunogold density showed that Shisa7 KO significantly reduced the density of GABA$_A$R α2 subunit (WT: n = 48/60; KO: n = 47/74, ****p < 0.0001, t test), and the number of GABA$_A$R α2 immunogold per synapse (WT: n = 43/50; KO: n = 46/64, *p < 0.05, t test). Scale bar, 200 nm for low magnification, 40 nm for high magnification. Data are mean ± S.E.M.

Figure. S14

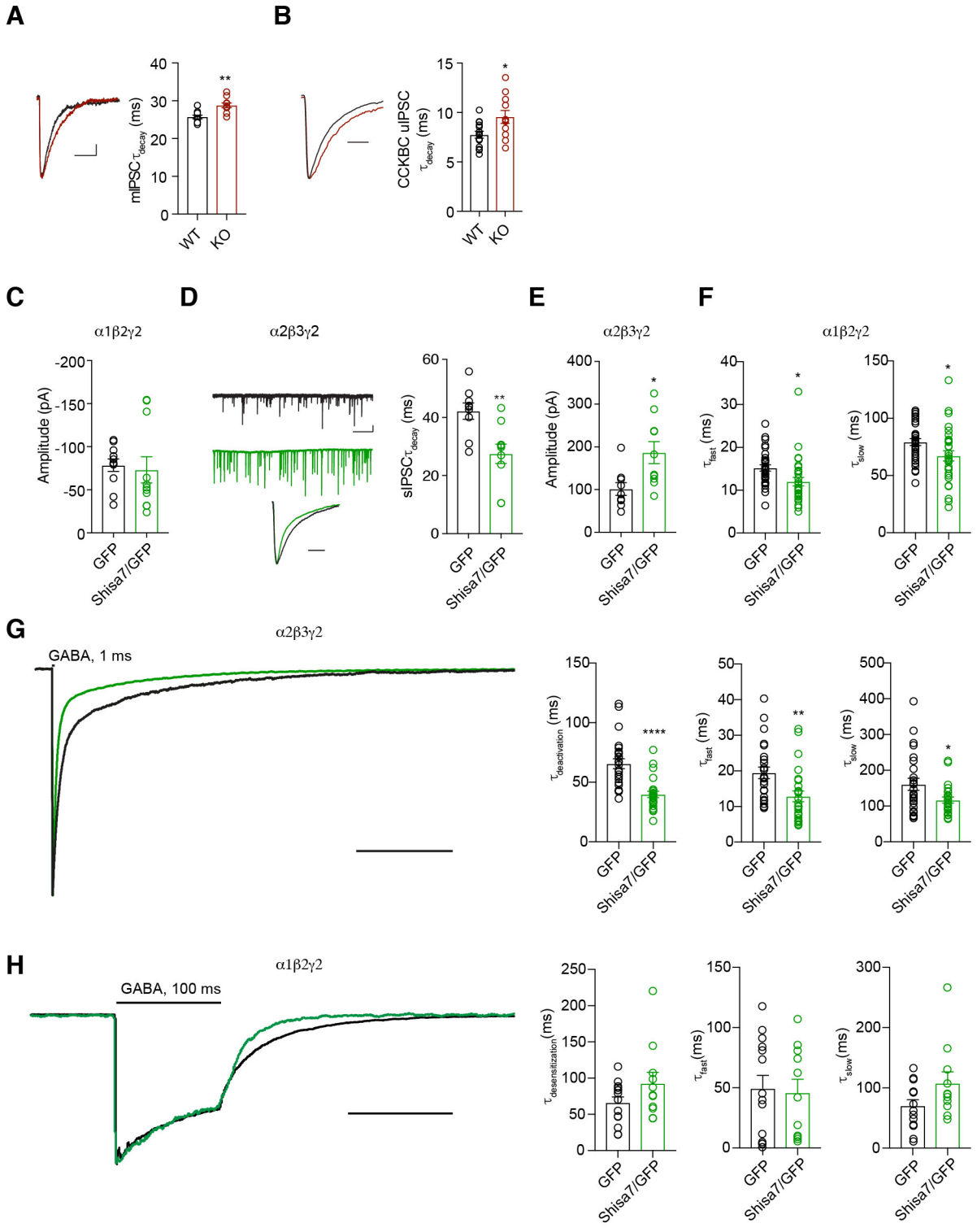

Fig. S14. Shisa7 speeds up $GABA_AR$ decay kinetics. (A) mIPSC decay time constant was significantly increased in Shisa7 KO CA1 neurons (WT: n = 10; KO: n = 10, **p* < 0.05, *t* test). Scale bar, 20 ms, 2 pA. **(B)** Shisa7 KO prolonged the decay time constant of CCKBC-CA1

pyramidal neuron uIPSCs (WT: n = 14, KO: n = 11; *p < 0.05, Mann-Whitney U test). Representative traces are peak normalized, scale bar, 5 ms. **(C)** Co-expression of Shisa7 did not change the amplitude of sIPSCs in HEK cells in co-culture expressing $\alpha1\beta2\gamma2$ (GFP: n = 11; Shisa7/GFP: n = 11, p = 0.75, t test). **(D)** Shisa7 significantly reduced the decay time constant of sIPSCs mediated by $\alpha2\beta3\gamma2$ (GFP: n = 9; Shisa7/GFP: n = 10, **p < 0.01, t test) in HEK cells in co-culture. Scale bar, 50 pA, 1 min. Peak-normalized sample traces were shown in the bottom. Scale bar, 100 ms. **(E)** Co-expression of Shisa7 significantly increased the amplitude of sIPSCs in HEK cells in co-cultures expressing $\alpha2\beta3\gamma2$ (GFP: n = 9; Shisa7/GFP: n = 10, *p < 0.05, t test). **(F)** Summary bar graphs of outside-out macro-patch recordings of currents mediated $\alpha1\beta2\gamma2$ receptors in response to 1 ms application of saturating GABA (5 mM) in HEK cells. The decay phase of the outside-out currents was fitted with a sum of two exponential curves. The values of the fast (τ_{fast}) and slow (τ_{slow}) components of $\alpha1\beta2\gamma2$ receptor deactivation time constants were significantly decreased in cells co-expressing Shisa7. (GFP: n = 31, Shisa7/GFP: n = 31, τ_{fast}: *p < 0.05; τ_{slow}: *p < 0.05, t test). **(G)** Peak-normalized sample traces from outside-out macro-patch recordings of currents mediated $\alpha2\beta3\gamma2$ receptors in response to 1 ms application of saturating GABA (5 mM) in HEK cells. The values of the weighted deactivation time constants, as well as the fast (τ_{fast}) and slow (τ_{slow}) components, were shown in the bar graphs. Shisa7 significantly reduced the weighted deactivation time constant (GFP: n = 25, Shisa7/GFP: n = 25, $\tau_{deactivation}$: ****p <0.0001; τ_{fast}: **p < 0.01; τ_{slow}: *p < 0.05, t test). Scale bar, 200 ms. **(H)** Peak-normalized sample traces from outside-out macro-patch recordings of currents mediated $\alpha1\beta2\gamma2$ receptors in response to 100 ms application of saturating GABA (5 mM) in HEK cells. The values of the weighted desensitization time constants, as well as the fast (τ_{fast}) and slow (τ_{slow}) components, were shown in the bar graphs. Shisa7 did not change the desensitization time constants (GFP: n = 15, Shisa7/GFP: n = 10, $\tau_{desensitization}$: p > 0.05; τ_{fast}: p > 0.05; τ_{slow}: p > 0.05, t test). Scale bar, 100 ms. Data are mean ± S.E.M.

Figure. S15

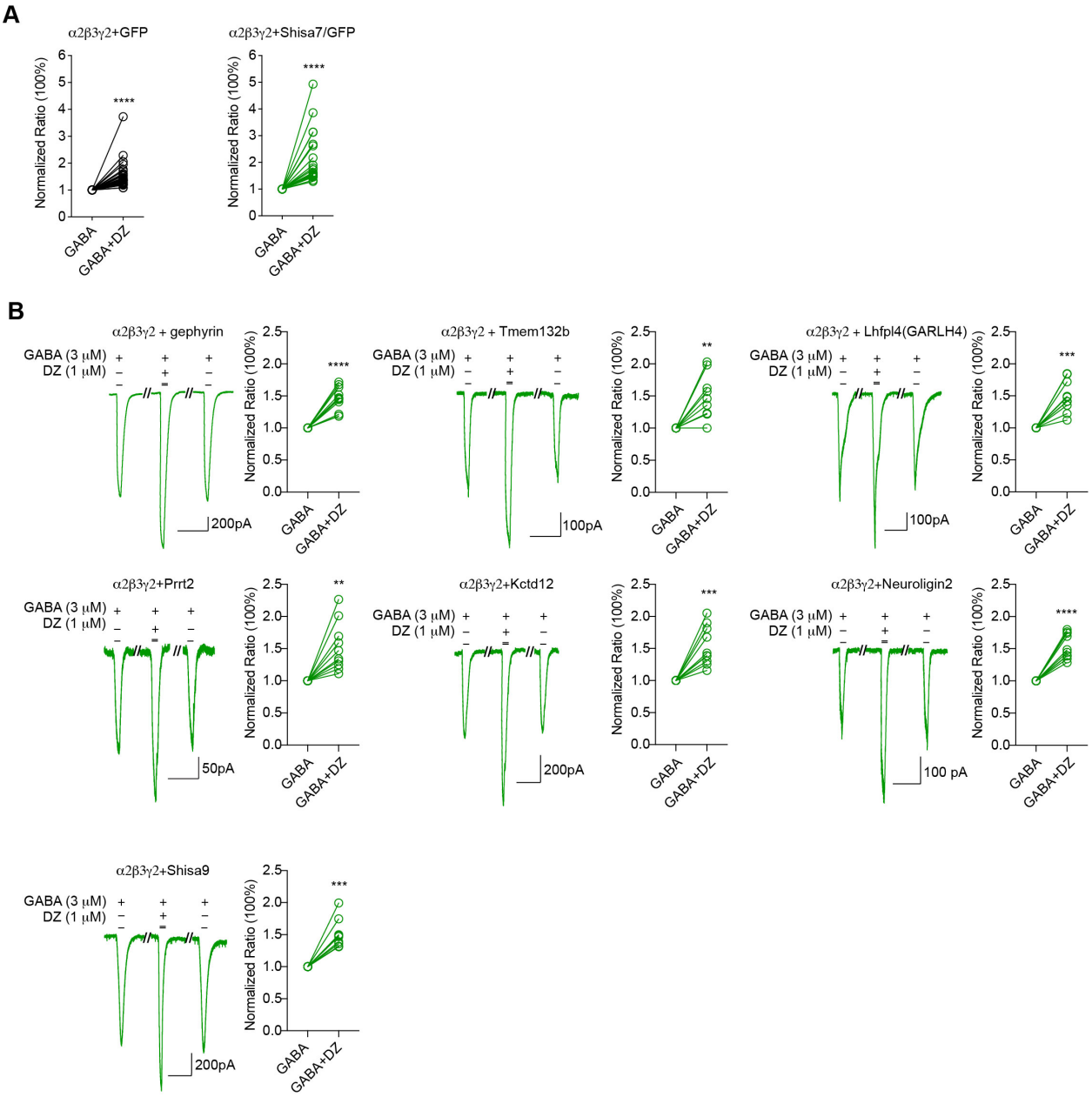

Fig. S15. Electrophysiological analysis of diazepam effect on $GABA_ARs$ in HEK cells. (A) DZ significantly potentiated GABA-evoked $GABA_AR$-mediated whole-cell currents in HEK cells expressing α2β3γ2 with GFP or with Shisa7/GFP (GFP: n = 32, ****p < 0.0001; Shisa7/GFP: n = 23; ****p < 0.0001, paired t test). **(B)** Sample traces of whole-cell currents in cells expressing α2β3γ2 together with indicated molecules evoked by GABA (3 μM) or GABA plus diazepam (1 μM, DZ). Bar graphs showed DZ-induced potentiation (gephyrin: n = 11; Tmem132b: n = 9; Lhfpl4(GARLH4): n = 10; Prrt2: n = 10; Kctd12: n = 10; Neuroligin2: n = 10; Shisa9: n = 9, ****p < 0.0001, ***p < 0.001, **p < 0.01; paired t test). Shisa9 was not shown to bind to $GABA_ARs$ and was used as a negative control for Shisa7. Scale bar, 10 s. Data are mean ± S.E.M.

Figure. S16

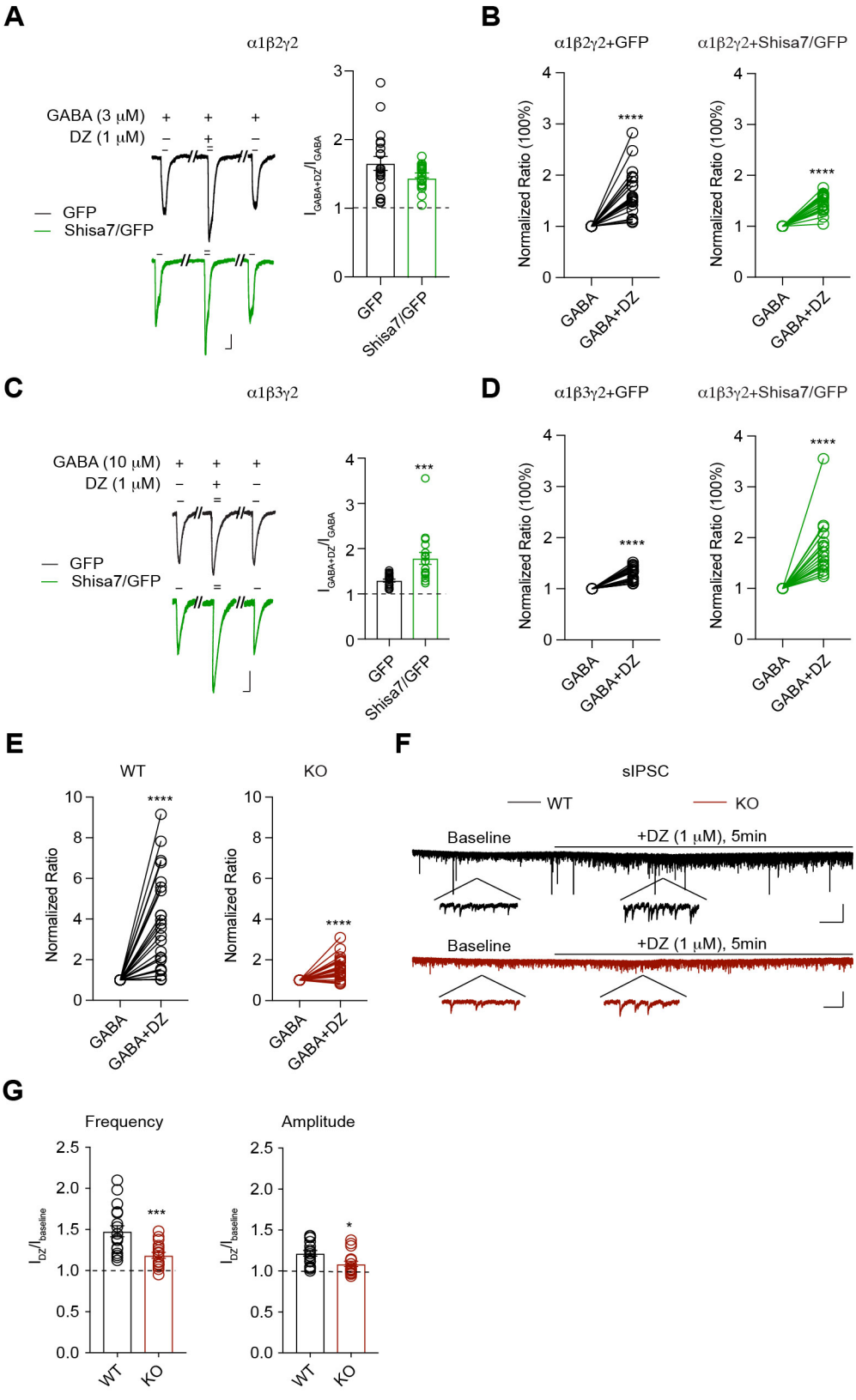
A
α1β2γ2
GABA (3 μM)
DZ (1 μM)
GFP
Shisa7/GFP
GFP
Shisa7/GFP
B
α1β2γ2+GFP
α1β2γ2+Shisa7/GFP
Normalized Ratio (100%)
GABA
GABA+DZ
C
α1β3γ2
GABA (10 μM)
DZ (1 μM)
D
α1β3γ2+GFP
α1β3γ2+Shisa7/GFP
E
WT
KO
Normalized Ratio
F
sIPSC
WT
KO
Baseline
+DZ (1 μM), 5min
G
Frequency
Amplitude
WT
KO

Fig. S16. Shisa7 modulates the action of diazepam on $GABA_A$Rs in both HEK cells and neurons. (A) Co-expression with Shisa7 did not significantly change DZ-induced potentiation in GABA (3 μM)-evoked $GABA_A$R-mediated whole-cell currents in HEK cells expressing $\alpha1\beta2\gamma2$ (GFP: n = 20, Shisa7/GFP: n = 23, $p > 0.05$, *t* test). Scale bar: 100 pA, 2 s. **(B)** DZ significantly potentiated GABA (3 μM, see Methods)-evoked $GABA_A$R-mediated whole-cell currents in HEK cells expressing $\alpha1\beta2\gamma2$ with GFP or Shisa7/GFP (GFP: n = 20, ****$p < 0.0001$; Shisa7/GFP: n = 23, ****$p < 0.0001$, paired *t* test). **(C)** Shisa7 significantly enhanced DZ-induced potentiation of responses to non-saturating GABA (10 μM) in HEK cells expressing $\alpha1\beta3\gamma2$ (GFP: n = 20; Shisa7/GFP: n = 18; ***$p < 0.001$, *t* test). Scale bar, 100 pA, 2 s. **(D)** DZ significantly potentiated GABA (10 μM, see Methods)-evoked $GABA_A$R-mediated whole-cell currents) in HEK cells expressing $\alpha1\beta3\gamma2$ with GFP or Shisa7/GFP (GFP: n = 20, ****$p < 0.0001$; Shisa7/GFP: n = 18, ****$p < 0.0001$, paired *t* test). **(E)** DZ (1 μM) significantly potentiated GABA (10 μM, see Methods)-evoked $GABA_A$R-mediated whole-cell currents in WT and Shisa7 KO hippocampal neuronal cultures (WT: n = 24, ****$p < 0.0001$; KO: n = 23, ****$p < 0.0001$, paired *t* test). **(F-G)** Sample traces showed that Shisa7 KO reduced DZ-mediated potentiation of sIPSCs in hippocampal CA1 pyramidal cells. Scale bar: top: 100 pA, 25 s; bottom: 50 pA, 0.5 s. The frequency and amplitude of sIPSCs were augmented by DZ (1 μM) in CA1 pyramidal neurons in acute hippocampal slices prepared from WT and Shisa7 KO mice. Shisa7 KO significantly reduced the DZ-induced enhancement of sIPSC frequency (WT: n = 18; KO: n = 17; ***$p < 0.001$, *t* test) and amplitude (WT: n = 18; KO: n = 17; *$p < 0.05$, *t* test) in CA1 pyramidal neurons in acute hippocampal slices. Data are mean ± S.E.M.

Figure. S17

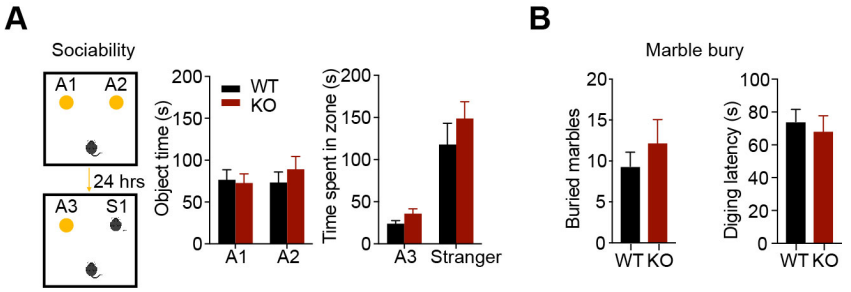

Fig. S17. Shisa7 KO does not change animals social and depression-like behaviors. (A) Shisa7 KO did not change the time spent in novelty zones and time spent in stranger zone (WT: n = 11; KO: n = 11, Two-way ANOVA with group (WT and KO), treatment (A1and A2) and interaction (object time: group: [$F_{1,42}$ = 0.216, p > 0.05]; treatment: [$F_{1,42}$ = 0.252, p > 0.05]; group x treatment: [$F_{1,42}$ = 0.560 p > 0.05]; Time in stranger zone: group: [$F_{1,42}$ = 39.69, ****p < 0.0001]; treatment: [$F_{1,42}$ = 1.679, p > 0.05]; group x treatment: [$F_{1,42}$ = 0.322, p > 0.05], Two-way ANOVA). **(B)** Shisa7 KO did not change the number of buried marbles and digging latency (WT: n = 6; KO: n = 6; numbers: p > 0.05; digging latency: p > 0.05, t test). Data are mean ± S.E.M.

Figure. S18

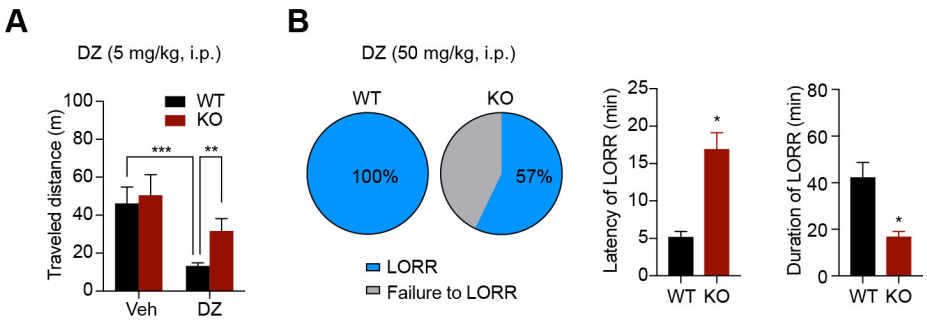

Fig. S18. Impairment of diazepam actions in Shisa7 KO mice
(A) DZ (5 mg/kg, i.p.) strongly reduced the traveled distance in open field test in WT group, but did not significantly decrease the traveled distance, although it trended lower, in KO group after 2-day habituation (Veh: WT: n = 5, KO: n = 10; DZ: WT: n = 10, KO: n = 8, treatment: [$F_{1,29}$ = 9.994, **p < 0.01]; group: [$F_{1,29}$ = 1.911, p > 0.05]; treatment x group: [$F_{1,29}$ = 0.746, p > 0.05], Two-way ANOVA). **(B)** DZ at the hypnotic dose produced LORR in 100% of WT mice (n = 6), but only in 57% of KO mice (4 out of 7 mice) under the treatment of DZ (50 mg/kg, i.p.). Shisa7 KO significantly prolonged latency to LORR and shortened duration of LORR after DZ administration (WT: n = 6, KO: n = 4 out of 7; *p < 0.05, *p < 0.05, t test). Data are mean ± S.E.M.

Movie S1

Vehicle. Mice were administrated with vehicle (i.p., 0.1 ml/10 g body weight), and the LORR latency and duration were tested. The behavior of a wild type (WT) mouse and a Shisa7 knockout (KO) mouse was recorded in the same screen. This video showed that both of Shisa7 WT and KO mice failed to exhibit LORR in 30 minutes, suggesting that vehicle did not induce LORR.

Movie S2

Diazepam (5 mg/ml, Hospira). Mice were administrated with diazepam (50 mg/kg, i.p., 0.1 ml/10 g body weight), and the LORR latency and duration were tested. The behavior of a WT mouse and a KO mouse were recorded in the same screen. The video showed that KO of Shisa7 prolonged LORR latency and reduced LORR duration compared to the WT mouse.

References and Notes

1. E. Sigel, M. E. Steinmann, Structure, function, and modulation of $GABA_A$ receptors. *J. Biol. Chem.* **287**, 40224–40231 (2012). doi:10.1074/jbc.R112.386664 Medline

2. R. W. Olsen, W. Sieghart, International Union of Pharmacology. LXX. Subtypes of γ-aminobutyric acid($_A$) receptors: Classification on the basis of subunit composition, pharmacology, and function. Update. *Pharmacol. Rev.* **60**, 243–260 (2008). doi:10.1124/pr.108.00505 Medline

3. T. C. Jacob, S. J. Moss, R. Jurd, GABA(A) receptor trafficking and its role in the dynamic modulation of neuronal inhibition. *Nat. Rev. Neurosci.* **9**, 331–343 (2008). doi:10.1038/nrn2370 Medline

4. B. Luscher, T. Fuchs, C. L. Kilpatrick, $GABA_A$ receptor trafficking-mediated plasticity of inhibitory synapses. *Neuron* **70**, 385–409 (2011). doi:10.1016/j.neuron.2011.03.024 Medline

5. M. Vithlani, M. Terunuma, S. J. Moss, The dynamic modulation of $GABA_A$ receptor trafficking and its role in regulating the plasticity of inhibitory synapses. *Physiol. Rev.* **91**, 1009–1022 (2011). doi:10.1152/physrev.00015.2010 Medline

6. M. Farrant, Z. Nusser, Variations on an inhibitory theme: Phasic and tonic activation of $GABA_A$ receptors. *Nat. Rev. Neurosci.* **6**, 215–229 (2005). doi:10.1038/nrn1625 Medline

7. R. W. Olsen, Allosteric ligands and their binding sites define γ-aminobutyric acid (GABA) type A receptor subtypes. *Adv. Pharmacol.* **73**, 167–202 (2015). doi:10.1016/bs.apha.2014.11.005 Medline

8. W. Sieghart, Allosteric modulation of GABAA receptors via multiple drug-binding sites. *Adv. Pharmacol.* **72**, 53–96 (2015). doi:10.1016/bs.apha.2014.10.002 Medline

9. W. Sieghart, M. M. Savić, International Union of Basic and Clinical Pharmacology. CVI: $GABA_A$ Receptor Subtype- and Function-selective Ligands: Key Issues in Translation to Humans. *Pharmacol. Rev.* **70**, 836–878 (2018). doi:10.1124/pr.117.014449 Medline

10. E. Engin, R. S. Benham, U. Rudolph, An Emerging Circuit Pharmacology of $GABA_A$ Receptors. *Trends Pharmacol. Sci.* **39**, 710–732 (2018). doi:10.1016/j.tips.2018.04.003 Medline

11. R. V. Klaassen, J. Stroeder, F. Coussen, A.-S. Hafner, J. D. Petersen, C. Renancio, L. J. M. Schmitz, E. Normand, J. C. Lodder, D. C. Rotaru, P. Rao-Ruiz, S. Spijker, H. D. Mansvelder, D. Choquet, A. B. Smit, Shisa6 traps AMPA receptors at postsynaptic sites and prevents their desensitization during synaptic activity. *Nat. Commun.* **7**, 10682 (2016). doi:10.1038/ncomms10682 Medline

12. J. von Engelhardt, V. Mack, R. Sprengel, N. Kavenstock, K. W. Li, Y. Stern-Bach, A. B. Smit, P. H. Seeburg, H. Monyer, CKAMP44: A brain-specific protein attenuating short-term synaptic plasticity in the dentate gyrus. *Science* **327**, 1518–1522 (2010). doi:10.1126/science.1184178 Medline

13. K. A. Pelkey, R. Chittajallu, M. T. Craig, L. Tricoire, J. C. Wester, C. J. McBain, Hippocampal GABAergic Inhibitory Interneurons. *Physiol. Rev.* **97**, 1619–1747 (2017). doi:10.1152/physrev.00007.2017 Medline

14. Y. Nakamura, D H. Morrow, A. Modgil, D. Huyghe, T. Z. Deeb, M. J. Lumb, P. A. Davies, S. J. Moss, Proteomic characterization of inhibitory synapses using a novel pHluorin-tagged γ-aminobutyric acid receptor, type A ($GABA_A$), α2 subunit knock-in mouse. *J. Biol. Chem.* **291**, 12394–12407 (2016). doi:10.1074/jbc.M116.724443.

15. E. A. Heller, W. Zhang, F. Selimi, J. C. Earnheart, M. A. Ślimak, J. Santos-Torres, I. Ibañez-Tallon, C. Aoki, B. T. Chait, N. Heintz, The biochemical anatomy of cortical inhibitory synapses. *PLOS ONE* **7**, e39572 (2012). doi:10.1371/journal.pone.0039572 Medline

16. T. Yamasaki, E. Hoyos-Ramirez, J. S. Martenson, M. Morimoto-Tomita, S. Tomita, GARLH Family Proteins Stabilize $GABA_A$ Receptors at Synapses. *Neuron* **93**, 1138–1152.e6 (2017). doi:10.1016/j.neuron.2017.02.023 Medline

17. E. C. Davenport, V. Pendolino, G. Kontou, T. P. McGee, D. F. Sheehan, G. López-Doménech, M. Farrant, J. T. Kittler, An Essential Role for the Tetraspanin LHFPL4 in the Cell-Type-Specific Targeting and Clustering of Synaptic $GABA_A$ Receptors. *Cell Reports* **21**, 70–83 (2017). doi:10.1016/j.celrep.2017.09.025 Medline

18. M. Wu, H.-L. Tian, X. Liu, J. H. C. Lai, S. Du, J. Xia, Impairment of Inhibitory Synapse Formation and Motor Behavior in Mice Lacking the NL2 Binding Partner LHFPL4/GARLH4. *Cell Reports* **23**, 1691–1705 (2018). doi:10.1016/j.celrep.2018.04.015 Medline

19. Y. Ge, Y. Kang, R. M. Cassidy, K.-M. Moon, R. Lewis, R. O. L. Wong, L. J. Foster, A. M. Craig, Clptm1 Limits Forward Trafficking of $GABA_A$ Receptors to Scale Inhibitory Synaptic Strength. *Neuron* **97**, 596–610.e8 (2018). doi:10.1016/j.neuron.2017.12.038 Medline

20. S. K. Tyagarajan, J. M. Fritschy, Gephyrin: A master regulator of neuronal function? *Nat. Rev. Neurosci.* **15**, 141–156 (2014). doi:10.1038/nrn3670 Medline

21. U. Rudolph, F. Crestani, D. Benke, I. Brünig, J. A. Benson, J.-M. Fritschy, J. R. Martin, H. Bluethmann, H. Möhler, Benzodiazepine actions mediated by specific γ-aminobutyric acid(A) receptor subtypes. *Nature* **401**, 796–800 (1999). doi:10.1038/44579 Medline

22. R. M. McKernan, T. W. Rosahl, D. S. Reynolds, C. Sur, K. A. Wafford, J. R. Atack, S. Farrar, J. Myers, G. Cook, P. Ferris, L. Garrett, L. Bristow, G. Marshall, A. Macaulay, N. Brown, O. Howell, K. W. Moore, R. W. Carling, L. J. Street, J. L. Castro, C. I. Ragan, G. R. Dawson, P. J. Whiting, Sedative but not anxiolytic properties of benzodiazepines are mediated by the $GABA_A$ receptor α1 subtype. *Nat. Neurosci.* **3**, 587–592 (2000). doi:10.1038/75761 Medline

23. K. Löw, F. Crestani, R. Keist, D. Benke, I. Brünig, J. A. Benson, J. M. Fritschy, T. Rülicke, H. Bluethmann, H. Möhler, U. Rudolph, Molecular and neuronal substrate for the selective attenuation of anxiety. *Science* **290**, 131–134 (2000). doi:10.1126/science.290.5489.131 Medline

24. F. Crestani, J. R. Martin, H. Möhler, U. Rudolph, Resolving differences in $GABA_A$ receptor mutant mouse studies. *Nat. Neurosci.* **3**, 1059 (2000). doi:10.1038/80553 Medline

25. M. P. Maher, J. A. Matta, S. Gu, M. Seierstad, D. S. Bredt, Getting a Handle on Neuropharmacology by Targeting Receptor-Associated Proteins. *Neuron* **96**, 989–1001 (2017). doi:10.1016/j.neuron.2017.10.001 Medline

26. P. Farrow, K. Khodosevich, Y. Sapir, A. Schulmann, M. Aslam, Y. Stern-Bach, H. Monyer, J. von Engelhardt, Auxiliary subunits of the CKAMP family differentially modulate AMPA receptor properties. *eLife* **4**, e09693 (2015). doi:10.7554/eLife.09693 Medline

27. L. J. M. Schmitz, R. V. Klaassen, M. Ruiperez-Alonso, A. E. Zamri, J. Stroeder, P. Rao-Ruiz, J. C. Lodder, R. J. van der Loo, H. D. Mansvelder, A. B. Smit, S. Spijker, The AMPA receptor-associated protein Shisa7 regulates hippocampal synaptic function and contextual memory. *eLife* **6**, e24192 (2017). doi:10.7554/eLife.24192 Medline

28. R. Baur, K. R. Tan, B. P. Lüscher, A. Gonthier, M. Goeldner, E. Sigel, Covalent modification of $GABA_A$ receptor isoforms by a diazepam analogue provides evidence for a novel benzodiazepine binding site that prevents modulation by these drugs. *J. Neurochem.* **106**, 2353–2363 (2008). doi:10.1111/j.1471-4159.2008.05574.x Medline

29. J. Ramerstorfer, R. Furtmüller, I. Sarto-Jackson, Z. Varagic, W. Sieghart, M. Ernst, The $GABA_A$ receptor α+β- interface: A novel target for subtype selective drugs. *J. Neurosci.* **31**, 870–877 (2011). doi:10.1523/JNEUROSCI.5012-10.2011 Medline

30. R. J. Walters, S. H. Hadley, K. D. Morris, J. Amin, Benzodiazepines act on $GABA_A$ receptors via two distinct and separable mechanisms. *Nat. Neurosci.* **3**, 1274–1281 (2000). doi:10.1038/81800 Medline

31. J. J. Quinlan, G. E. Homanics, L. L. Firestone, Anesthesia sensitivity in mice that lack the β3 subunit of the γ-aminobutyric acid type A receptor. *Anesthesiology* **88**, 775–780 (1998). doi:10.1097/00000542-199803000-00030 Medline

32. M. K. Mulligan, T. Abreo, S. M. Neuner, C. Parks, C. E. Watkins, M. T. Houseal, T. M. Shapaker, M. Hook, H. Tan, X. Wang, J. Ingels, J. Peng, L. Lu, C. C. Kaczorowski, C. D. Bryant, G. E. Homanics, R. W. Williams, Identification of a Functional Non-coding Variant in the GABA $_A$ Receptor α2 Subunit of the C57BL/6J Mouse Reference Genome: Major Implications for Neuroscience Research. *Front. Genet.* **10**, 188 (2019). doi:10.3389/fgene.2019.00188 Medline

33. J. E. Kralic, T. K. O'Buckley, R. T. Khisti, C. W. Hodge, G. E. Homanics, A. L. Morrow, $GABA_A$ receptor alpha-1 subunit deletion alters receptor subtype assembly, pharmacological and behavioral responses to benzodiazepines and zolpidem. *Neuropharmacology* **43**, 685–694 (2002). doi:10.1016/S0028-3908(02)00174-0 Medline

34. Y. A. Blednov, S. Jung, H. Alva, D. Wallace, T. Rosahl, P.-J. Whiting, R. A. Harris, Deletion of the α1 or β2 subunit of $GABA_A$ receptors reduces actions of alcohol and other drugs. *J. Pharmacol. Exp. Ther.* **304**, 30–36 (2003). doi:10.1124/jpet.102.042960 Medline

35. U. Rudolph, B. Antkowiak, Molecular and neuronal substrates for general anaesthetics. *Nat. Rev. Neurosci.* **5**, 709–720 (2004). doi:10.1038/nrn1496 Medline

36. A. C. Jackson, R. A. Nicoll, The expanding social network of ionotropic glutamate receptors: TARPs and other transmembrane auxiliary subunits. *Neuron* **70**, 178–199 (2011). doi:10.1016/j.neuron.2011.04.007 Medline

37. E. Jacobi, J. von Engelhardt, Diversity in AMPA receptor complexes in the brain. *Curr. Opin. Neurobiol.* **45**, 32–38 (2017). doi:10.1016/j.conb.2017.03.001 Medline

38. C. Straub, S. Tomita, The regulation of glutamate receptor trafficking and function by TARPs and other transmembrane auxiliary subunits. *Curr. Opin. Neurobiol.* **22**, 488–495 (2012). doi:10.1016/j.conb.2011.09.005 Medline

39. I. H. Greger, J. F. Watson, S. G. Cull-Candy, Structural and Functional Architecture of AMPA-Type Glutamate Receptors and Their Auxiliary Proteins. *Neuron* **94**, 713–730 (2017). doi:10.1016/j.neuron.2017.04.009 Medline

40. W. Han, H. Wang, J. Li, S. Zhang, W. Lu, Ferric Chelate Reductase 1 Like Protein (FRRS1L) Associates with Dynein Vesicles and Regulates Glutamatergic Synaptic Transmission. *Front. Mol. Neurosci.* **10**, 402 (2017). doi:10.3389/fnmol.2017.00402 Medline

41. X. Gu, X. Mao, M. P. Lussier, M. A. Hutchison, L. Zhou, F. K. Hamra, K. W. Roche, W. Lu, GSG1L suppresses AMPA receptor-mediated synaptic transmission and uniquely modulates AMPA receptor kinetics in hippocampal neurons. *Nat. Commun.* **7**, 10873 (2016). doi:10.1038/ncomms10873 Medline

42. Y. S. Yim, Y. Kwon, J. Nam, H. I. Yoon, K. Lee, D. G. Kim, E. Kim, C. H. Kim, J. Ko, Slitrks control excitatory and inhibitory synapse formation with LAR receptor protein tyrosine phosphatases. *Proc. Natl. Acad. Sci. U.S.A.* **110**, 4057–4062 (2013). doi:10.1073/pnas.1209881110 Medline

43. R. Sando, X. Jiang, T. C. Südhof, Latrophilin GPCRs direct synapse specificity by coincident binding of FLRTs and teneurins. *Science* **363**, eaav7969 (2019). doi:10.1126/science.aav7969 Medline

44. K. W. Dunn, M. M. Kamocka, J. H. McDonald, A practical guide to evaluating colocalization in biological microscopy. *Am. J. Physiol. Cell Physiol.* **300**, C723–C742 (2011). doi:10.1152/ajpcell.00462.2010 Medline

45. P. R. Dunkley, P. E. Jarvie, P. J. Robinson, A rapid Percoll gradient procedure for preparation of synaptosomes. *Nat. Protoc.* **3**, 1718–1728 (2008). doi:10.1038/nprot.2008.171 Medline

46. F. Viennot, J. C. Artault, G. Tholey, J. De Barry, G. Gombos, An improved method for the preparation of rat cerebellar glomeruli. *J. Neurosci. Methods* **38**, 51–62 (1991). doi:10.1016/0165-0270(91)90154-R Medline

47. G. Maksay, S. A. Thompson, K. A. Wafford, Allosteric modulators affect the efficacy of partial agonists for recombinant GABA($_A$) receptors. *Br. J. Pharmacol.* **129**, 1794–1800 (2000). doi:10.1038/sj.bjp.0703259 Medline

48. R. T. Robinson, B. C. Drafts, J. L. Fisher, Fluoxetine increases $GABA_A$ receptor activity through a novel modulatory site. *J. Pharmacol. Exp. Ther.* **304**, 978–984 (2003). doi:10.1124/jpet.102.044834 Medline

49. S. Hannan, M. Mortensen, T. G. Smart, Snake neurotoxin α-bungarotoxin is an antagonist at native $GABA_A$ receptors. *Neuropharmacology* **93**, 28–40 (2015). doi:10.1016/j.neuropharm.2015.01.001 Medline

50. J. A. Benson, K. Löw, R. Keist, H. Mohler, U. Rudolph, Pharmacology of recombinant γ-aminobutyric acid$_A$ receptors rendered diazepam-insensitive by point-mutated α-subunits. *FEBS Lett.* **431**, 400–404 (1998). doi:10.1016/S0014-5793(98)00803-5 Medline

51. A. T. Che Has, N. Absalom, P. S. van Nieuwenhuijzen, A. N. Clarkson, P. K. Ahring, M. Chebib, Zolpidem is a potent stoichiometry-selective modulator of α1β3 GABA$_A$ receptors: Evidence of a novel benzodiazepine site in the α1-α1 interface. *Sci. Rep.* **6**, 28674 (2016). doi:10.1038/srep28674 Medline

52. M. Jonsson Fagerlund, J. Sjödin, J. Krupp, M. A. Dabrowski, Reduced effect of propofol at human α1β2(N289M)γ2 and α2β3(N290M)γ2 mutant GABA$_A$ receptors. *Br. J. Anaesth.* **104**, 472–481 (2010). doi:10.1093/bja/aeq023 Medline

53. N. Karim, P. Wellendorph, N. Absalom, G. A. R. Johnston, J. R. Hanrahan, M. Chebib, Potency of GABA at human recombinant GABA$_A$ receptors expressed in Xenopus oocytes: A mini review. *Amino Acids* **44**, 1139–1149 (2013). doi:10.1007/s00726-012-1456-y Medline

54. C. Dixon, P. Sah, J. W. Lynch, A. Keramidas, GABA$_A$ receptor α and γ subunits shape synaptic currents via different mechanisms. *J. Biol. Chem.* **289**, 5399–5411 (2014). doi:10.1074/jbc.M113.514695 Medline

55. M. S. Wyeth, K. A. Pelkey, X. Yuan, G. Vargish, A. D. Johnston, S. Hunt, C. Fang, D. Abebe, V. Mahadevan, A. Fisahn, M. W. Salter, R. R. McInnes, R. Chittajallu, C. J. McBain, Neto Auxiliary Subunits Regulate Interneuron Somatodendritic and Presynaptic Kainate Receptors to Control Network Inhibition. *Cell Reports* **20**, 2156–2168 (2017). doi:10.1016/j.celrep.2017.08.017 Medline

56. L. Cathala, N. B. Holderith, Z. Nusser, D. A. DiGregorio, S. G. Cull-Candy, Changes in synaptic structure underlie the developmental speeding of AMPA receptor-mediated EPSCs. *Nat. Neurosci.* **8**, 1310–1318 (2005). doi:10.1038/nn1534 Medline

57. R. S. Petralia, Y. X. Wang, F. Hua, Z. Yi, A. Zhou, L. Ge, F. A. Stephenson, R. J. Wenthold, Organization of NMDA receptors at extrasynaptic locations. *Neuroscience* **167**, 68–87 (2010). doi:10.1016/j.neuroscience.2010.01.022 Medline

58. R. S. Petralia, R. J. Wenthold, Immunocytochemistry of NMDA receptors. *Methods Mol. Biol.* **128**, 73–92 (1999). Medline

59. S. Viswanathan, M. E. Williams, E. B. Bloss, T. J. Stasevich, C. M. Speer, A. Nern, B. D. Pfeiffer, B. M. Hooks, W.-P. Li, B. P. English, T. Tian, G. L. Henry, J. J. Macklin, R. Patel, C. R. Gerfen, X. Zhuang, Y. Wang, G. M. Rubin, L. L. Looger, High-performance probes for light and electron microscopy. *Nat. Methods* **12**, 568–576 (2015). doi:10.1038/nmeth.3365 Medline

60. T. Wang, W. Han, A. S. Chitre, O. Polesskaya, L. C. Solberg Woods, A. A. Palmer, H. Chen, Social and anxiety-like behaviors contribute to nicotine self-administration in adolescent outbred rats. *Sci. Rep.* **8**, 18069 (2018). doi:10.1038/s41598-018-36263-w Medline

61. N. P. Franks, General anaesthesia: From molecular targets to neuronal pathways of sleep and arousal. *Nat. Rev. Neurosci.* **9**, 370–386 (2008). doi:10.1038/nrn2372 Medline

62. C. Ruzza, A. Rizzi, D. Malfacini, A. Pulga, S. Pacifico, S. Salvadori, C. Trapella, R. K. Reinscheid, G. Calo, R. Guerrini, In vitro and in vivo pharmacological characterization of a neuropeptide S tetrabranched derivative. *Pharmacol. Res. Perspect.* **3**, e00108 (2015). doi:10.1002/prp2.108 Medline